Constitutive androstane receptor directs T cell adaptation to bile acids in the small intestine

Mei Lan Chen[1#], Xiangsheng Huang[2#], Hongtao Wang[2], Yujin Liu[1], Jinsai Shang[3], Amber Eliason[1], Courtney Hegner[1], HaJeung Park[4], Blake Frey[5], Guohui Wang[2], Douglas J. Kojetin[3,6], Casey T. Weaver[5], Matthew E. Pipkin[1], David D. Moore[7]*, and Mark S. Sundrud[1]*

[1]Department of Immunology and Microbiology, The Scripps Research Institute, Jupiter, FL 33458, USA

[2]Department of Pediatrics, Section of Gastroenterology, Baylor College of Medicine and Texas Children's Hospital, Houston, TX, 77030, USA

[3]Department of Integrative Structural and Computational Biology, The Scripps Research Institute, Jupiter, FL 33458, USA

[4]X-ray Crystallography Core Facility, The Scripps Research Institute, Jupiter, FL 33458, USA

[5]Department of Pathology, University of Alabama at Birmingham, Birmingham, AL 35203, USA

[6]Department of Molecular Medicine, The Scripps Research Institute, Jupiter, FL 33458, USA

[7]Department of Molecular and Cellular Biology, Baylor College of Medicine, 1 Baylor Plaza, Houston, Texas 77030, USA

[#]Equal contribution

***Correspondence: David D. Moore (moore@bcm.edu), Mark S. Sundrud (msundrud@scripps.edu)

Key words: IBD, T cells, Th1, Th17, bile acids, MDR1, CAR, NR1I3, Xenobiotics

Abbreviations: MDR1, multidrug resistance 1; TNFα, tumor necrosis factor alpha; IFNγ, interferon gamma; IL-10, interleukin-10; IL-17, interleukin-17; TCR, T cell receptor; *Abcb1a*, ATP-binding cassette subfamily B, member 1a; *Abcb1b*, ATP-binding cassette subfamily B, member 1b; *Rag1*, recombination-activating gene 1; *Rag2*, recombination-activating gene 2.

Bile acids (BAs) are fundamental lipid emulsifying metabolites synthesized in hepatocytes and maintained via enterohepatic circulation between the liver and ileum[1]. Because they are lipophilic, BAs can be cytotoxic in enterohepatic tissues[2] and several nuclear receptors are now recognized for suppressing BA toxicity in hepatocytes and enterocytes[3]. By contrast, it remains unclear how mucosal immune cells protect themselves from high BA concentrations in the small intestine. We previously showed that CD4$^+$ T effector (Teff) cells upregulate expression of the xenobiotic transporter, MDR1, in the ileum to prevent BA toxicity and suppress Crohn's disease-like small bowel inflammation[4]. Here, we identify the BA- and xenobiotic-sensing nuclear receptor, constitutive androstane receptor (CAR/*NR1I3*)[5], as a regulator of MDR1 expression in mucosal T cells. CAR expression increased in Teff cells during mucosal inflammation and promoted large-scale transcriptional reprogramming in the small intestine lamina propria (siLP). CAR-dependent gene expression in siLP Teff cells shared features with that in hepatocytes, and involved the induction of detoxifying enzymes and transporters, but also the key anti-inflammatory cytokine, *Il10*. CAR-deficiency in Teff cells exacerbated, whereas pharmacologic CAR activation suppressed, BA-driven ileitis in T cell-reconstituted *Rag*$^{-/-}$ mice. In addition, bile, though not major BA species *per se*, enhanced CAR transcriptional activity, and CAR-dependent gene expression in human CD4$^+$ Th cells was restricted to $\alpha4^+\beta7^+$CCR9$^+$ Teff cells licensed for small bowel homing. These data implicate CAR in prompting a hepatocyte-like transcriptional response in mucosal T cells that detoxifies BAs and enforces small bowel immune homeostasis. Pharmacologic activation of this program may offer an unexpected strategy to treat small bowel Crohn's disease.

In seeking to define the transcriptional mechanisms that promote MDR1 upregulation in siLP Teff cells and safeguard small bowel immune homeostasis in the presence of BAs[4], we considered the role of ligand-regulated nuclear receptors (NRs), which act as environmental sensors to regulate diverse gene expression programs important for immunity, inflammation, metabolism and gastrointestinal physiology[6]. To test the contribution of all 49 mouse NRs to MDR1 regulation in siLP Teff cells, we performed a pooled *in vivo* RNAi screen using MDR1-dependent rhodamine 123 (Rh123) efflux as a readout[7]. FVB wild type naïve CD4$^+$ T cells were activated and transduced *in vitro* with a library of 258 mouse retroviruses carrying unique shRNAmirs against 70 genes together with the fluorescent reporter, ametrine[8] (**Fig. 1a**, Extended Data Fig. 1). In addition to NRs, this library included shRNAmirs against 10 major NR co-activators and co-repressors, the aryl hydrocarbon receptor (AhR), the cell-surface BA receptor Takeda G-coupled protein receptor 5 (Tgr5; encoded by *Gpbar1*)[9] and a downstream transcription factor (*Creb1*), as well as a number of positive (*Abcb1a*, *Abcb1b*) and negative (*Cd8a*, *Cd19*, *EGFP*, *RFP*) control genes (Extended Data Fig. 1). Separately-transduced T cells were pooled, FACS-sorted for ametrine expression and transplanted into syngeneic *Rag1*$^{-/-}$ mice. Six weeks later, transduced Teff cells (CD4$^+$CD25$^-$CD62L^{lo}CD44^{hi}ametrine$^+$) were FACS-sorted from the spleen or siLP,

and portions of these cells were divided into MDR1^{hi} or MDR1^{lo} subsets based on *ex vivo* Rh123 efflux; relative shRNAmir abundances within each cell pool were quantified by DNA-seq (**Fig. 1a**).

Three sets of shRNAmirs—against thyroid hormone receptor alpha (*Thra*), estrogen related receptor alpha (*Esrra*), and constitutive androstane receptor (CAR/*Nr1i3*)—were most strongly and consistently enriched in MDR1^{lo} *vs*. MDR1^{hi} Teff cells from both spleen and siLP, similar to shRNAmirs against MDR1 (*Abcb1a*) itself, and after excluding 36 shRNAmirs that either markedly reduced Teff cell persistence *in vivo* or were poorly represented (before and after *in vivo* transfer) (**Fig. 1b-c**; Extended Data Fig. 2a). This suggested that *Thra, Esrra* and CAR/*Nrli3* might each be positive regulators of MDR1 expression, although none of these NRs have reported functions in T cells. We prioritized CAR for validation because it is known for protecting hepatocytes from drug- and BA-induced toxicity[5,10] and has been implicated in regulating hepatic MDR1 expression[11]. Individual gene depletion experiments confirmed that 3 of the 5 CAR-targeting shRNAmirs reduced MDR1-dependent Rh123 efflux in Teff cells recovered from transferred *Rag1*$^{-/-}$ mice (**Fig. 1d-e**, Extended Data Fig. 2b-c). These same constructs diminished MDR1 (*Abcb1a*) and CAR (*Nr1i3*) gene expression, as judged by qPCR, as well as expression of the signature CAR transcriptional target, *Cyp2b10*[12] (Extended Data Fig. 2d).

CAR binds to DNA and regulates gene expression as a heterodimer with retinoid X receptors (RXRα/β/γ). However, RXRs also dimerize with many other NRs, including retinoic acid receptors (RARα/β/γ), peroxisome proliferator-activated receptors (PPARα/δ/γ) and vitamin D receptor (VDR), all of which regulate diverse aspects of T cell function *in vivo*[13]. Consistent with this broader function, shRNAmir-mediated depletion of RXRα—the major RXR isoform expressed in T cells—did not selectively regulate MDR1 expression, but rather impaired persistence of circulating Teff cells *in vivo* (Extended Data Fig. 2e). Depletion of the CAR-related xenobiotic-sensor, pregnane X receptor (PXR)[14], influenced neither Teff cell persistence nor MDR1 expression *in vivo* (**Fig. 1b-c**; Extended Data Fig. 2e). Consistent with this result, Teff cells from C57BL/6 (B6)-derived CAR-deficient (*Nr1i3*$^{-/-}$) mice[12] displayed lower MDR1-dependent Rh123 efflux and *Abcb1a* mRNA expression than those from PXR-deficient (*Nr1i2*$^{-/-}$) mice[15], after co-transfer into *Rag1*$^{-/-}$ mice together with CD45.1 wild type cells; Teff cells lacking both CAR and PXR[10] showed equivalently low MDR1 expression as those lacking only CAR (Extended Data Fig. 3). These data implicate CAR in the regulation of mucosal CD4^{+} T cell function.

In the standard T cell transfer model of inflammatory bowel disease[16], introduction of naïve CD4^{+} T cells into immunodeficient hosts results in progressive colitis with little involvement of the small intestine. By contrast, we have previously reported that T cells lacking MDR1 (*Abcb1a*$^{-/-}$*Abcb1b*$^{-/-}$) on the FVB background induce both colitis and BA-driven ileitis upon transfer into syngeneic *Rag1*$^{-/-}$ mice[4]. In line with these results, shRNAmir-mediated CAR depletion in FVB wild type T cells exacerbated T cell transfer-induced weight loss in *Rag1*$^{-/-}$ mice, and did so in a manner that correlated directly with the degree of MDR1 down-regulation in

these cells (**Fig. 1e**; Extended data Fig. 1b-d). Similarly, naive Th cells from C57BL/6 (B6)-derived CAR-deficient (*Nr1i3*$^{-/-}$) mice induced more severe weight loss and ileitis than wild type counterparts, but not colitis, after transfer into *Rag2*$^{-/-}$ mice co-housed to normalize microflora (**Fig. 1f-g**). Therapeutic administration of the BA sequestering resin, cholestyramine (CME), which binds BAs in the lumen of the small intestine and prevents reabsorption into the ileal mucosa[17], normalized weight loss and ileitis between *Rag2*$^{-/-}$ mice receiving CAR-sufficient or CAR-deficient T cells (Extended Data Fig. 4a-b); as did ablation of the ileal BA reuptake transporter, Apical sodium-dependent BA transporter (Asbt/*Slc10a2*) in reconstituted *Rag1*$^{-/-}$ mice (Extended Data Fig. 4c-d). These results suggest that CAR acts in mucosal T cells to enforce small bowel immune homeostasis, and that loss of CAR exacerbates ileitis that is not transmissible by microbiota and requires BA reabsorption.

To elucidate the gene regulatory networks governed by CAR in mucosal Teff cells *in vivo*, we used RNA-seq to analyze the transcriptomes of wild type and CAR-deficient Teff cells in spleen, siLP and colon lamina propria (cLP) of congenically co-transferred *Rag1*$^{-/-}$ mice—where CD45.1^{+} CAR-sufficient and CD45.2^{+} CAR-deficient Teff cells are present in the same animals as tissue bystanders (**Fig. 2a**). Wild type Teff cell gene expression differed substantially in spleen, siLP and cLP, and CAR-deficiency most prominently altered gene expression in the small intestine (**Fig. 2b-c**). siLP Teff cells lacking CAR failed to upregulate dozens of 'siLP-signature' genes (*i.e.*, genes increased in wild type siLP Teff cells, compared with counterparts from either spleen or colon) (**Fig. 2c-d**, Extended Data Fig. 5a). CAR-dependent siLP-signature genes in Teff cells were enriched for those induced by CAR in mouse hepatocytes after *in vivo* administration of the selective small molecule CAR agonist, 1,4-*Bis*(3,5-Dichloro-2-pyridinyloxy) benzene (TC)[18,19] (**Fig. 2d**, Extended Data Fig. 5b-c). Genes displaying CAR-dependent regulation in both siLP Teff cells and hepatocytes were further enriched for loci at which TC-inducible CAR-occupancy was seen by ChIP-seq in hepatocytes[20] (Extended Data Fig. 5d). In addition to MDR1/*Abcb1a* and *Cyp2b10*, putative CAR transcriptional targets shared between mucosal Teff cells and hepatocytes included additional ATP-binding cassette (ABC)-containing transporters (*e.g.*, *Abcb4*) and cytochrome P450 enzymes (*e.g.*, *Cyp2r1*) (Extended Data Fig. 5e). Consistent with the regulation of a cytoprotective transcriptional program, Teff cells lacking CAR displayed impaired persistence *in vivo*, most immediately in the small intestine (Extended Data Fig. 6a-d).

CAR-deficient siLP Teff cells displayed reduced expression of genes ascribed to Foxp3^{-}IL-10^{+} type 1 regulatory (Tr1) cells[21] (**Fig. 2d**), a key immunoregulatory T cell subset known to suppress mucosal inflammation in humans and mice[22,23]. Consistently, CAR-deficient Teff cells recovered from transferred *Rag1*$^{-/-}$ mice showed a near-complete loss of IL-10 production, but normal pro-inflammatory cytokine (IFNγ, TNFα) expression, after *ex vivo* stimulation (**Fig. 2e-f**, data not shown). CAR-dependent IL-10 expression was evident in siLP, as well as spleen and mesenteric lymph nodes (MLN), but was conspicuously absent in the colon (**Fig. 2e-f**, Extended Data Fig. 6e-g). CAR-dependent IL-10 production was also transient—peaking 2-weeks after

donor T cell engraftment and waning thereafter—and followed the kinetics of both donor Teff cell infiltration into siLP of recipient mice and *ex vivo* CAR (*Nr1i3*) gene expression (Extended Data Fig. 7a-c). Conversely, Th17-signature genes[24], although not *Il17a* itself, were elevated in siLP Teff cells lacking CAR (**Fig. 2d**); reduced IL-10 production in the absence of CAR paralleled accumulation of RORγt^{+}IL-17A^{-} 'poised' Th17 cells[25,26] in siLP (Extended Data Fig. 7d-e). Together, these data suggest that CAR acts early in the T cell response to small bowel injury by activating diverse gene expression programs that detoxify BAs, promote the Tr1 phenotype, limit Th17 cell accumulation and foster inflammation-resolution. CAR was also required for IL-10 expression in endogenous siLP effector and regulatory subsets from B6 mice injected with anti-CD3 antibodies to induce mucosal inflammation[27] (Extended data Figure 8).

If loss of CAR in Teff cells exacerbates BA-driven small bowel inflammation, we reasoned that pharmacologic CAR activation might be protective. Administration of the selective CAR agonist, TC, to congenically co-transferred *Rag1*$^{-/-}$ mice induced *Abcb1a*, *Cyp2b10* and *Il10* upregulation in wild type, but not CAR-deficient, Teff cells (**Fig. 2g**). *In vivo* TC treatment also reduced ileitis, but not colitis, in *Rag2*$^{-/-}$ mice reconstituted with only wild type T cells and fed a standard 2% cholic acid (CA)-supplemented diet to increase BA-driven small bowel injury[28] (**Fig. 2h-i**); CA-feeding increased morbidity and mortality in *Rag2*$^{-/-}$ mice receiving wild type T cells, but had no obvious effects on *Rag2*$^{-/-}$ mice in the absence of T cell transfer (**Fig. 2h**, data not shown). In addition, protective effects of TC treatment in this model were lost in CA-fed *Rag2*$^{-/-}$ mice reconstituted with CAR-deficient T cells (Extended Data Fig. 9a-c). These results suggest that CA-feeding can promote, whereas T cell-intrinsic CAR activation can suppress, small bowel inflammation *in vivo*, although we cannot exclude additional effects stemming from TC-mediated CAR activation in other host cell types (*e.g.*, hepatocytes, enterocytes). TC, but not a PXR agonist, 5-Pregnen-3β-ol-20-one-16α-carbonitrile (PCN)[29], also prompted CAR-dependent *Abcb1a*, *Cyp2b10* and *Il10* upregulation in *ex vivo*-stimulated wild type Teff cells from spleens of transferred *Rag1*$^{-/-}$ mice; *ex vivo* effects TC treatment were dose-dependent between 5-20 μM, and blocked by the CAR inverse agonist, 5α-Androstan-3β-ol[10] (Extended Data Figure 9d-g).

Preferential CAR activity in siLP Teff cells *in vivo* suggested the possibility of CAR activation by endogenous intestinal metabolites. To examine this, we developed a recombinant protein-based activity assay, in which ligand-induced recruitment of a co-activator peptide (PGC1α) to activated CAR-RXR ligand-binding domain (LBD) heterodimers was quantified by time-resolved fluorescence resonance energy transfer (TR-FRET) (**Fig. 3a**). Both bile (from gallbladder) and sterile, soluble small intestine lumen content (siLC) from wild type B6 mice—but not colon lumen content (cLC) or serum—activated CAR-RXR LBD heterodimers in a dose-dependent manner, similar to TC (**Fig. 3a-b**). These same extracts failed to activate RXR LBD homodimers, suggesting direct interaction with the CAR LBD (**Fig. 3b**); we were not able to purify CAR LBD from bacteria in the absence of RXR LBD, as it was insoluble and partitioned into exclusion bodies (data not shown). Concentrations of bile and siLC that activated CAR LBD in TR-FRET experiments also induced CAR-

dependent *Abcb1a*, *Cyp2b10* and *Il10* upregulation in *ex vivo*-stimulated wild type, but not CAR-deficient, Teff cells from transferred *Rag1*$^{-/-}$ spleens (**Fig. 3c**). CAR activation was equivalent between siLC isolated from conventionally-housed and germ-free (GF) wild type mice, and was also unaffected by CME-mediated depletion of free BAs[4] (**Fig. 3d**). In line with this result, no commercially-available BA species were sufficient to activate CAR-RXR LBD heterodimers in TR-FRET experiments, or to stimulate CAR-dependent gene expression in *ex vivo*-cultured Teff cells (Extended Data Fig. 10a, data not shown). These results suggest that CAR activity may be enhanced in siLP Teff cells through local interactions with either non-BA components in bile, or less abundant BA species, which circulate enterohepatically between the liver and small intestine. This is consistent with current paradigms that CAR is indirectly activated in the presence of BAs, but does not bind major BA species directly[30]. Intriguingly, CAR activation by siLC from T cell-reconstituted *Rag1*$^{-/-}$ mice decreased steadily over the course of intestinal inflammation, whereas CAR activation by cLC of these same animals increased over time (Extended Data Fig. 10b). Thus, mucosal inflammation may decrease the abundance of endogenous CAR-activating metabolites in the small intestine, akin to the influence of mucosal inflammation on BA malabsorption[31].

Finally, we sought to establish the relevance of CAR in human T cells. Considering its preferential activity in mouse siLP Teff cells, we reasoned that CAR expression and function in human peripheral blood T cells might be enriched within subsets of circulating Teff cells that express the small bowel-homing receptors, α4β7 integrin and CCR9[32], and are thus more likely to have recently recirculated from siLP. A small but reliable subset of $\alpha4^+\beta7^+CCR9^+$ Teff cells (~ 1-5%) was detected in peripheral blood from healthy adults (**Fig. 4a-c**). Expression of these small bowel-homing receptors was absent on naïve $CD4^+$ T cells, as expected, and reduced among circulating $CD25^+$ T regulatory (Treg) cells (**Fig. 4a-c**), suggesting that Treg cells may be retained in the intestinal mucosa more effectively than Teff cells. Given the lack of specific CAR antibodies, we assessed CAR function in human T cell subsets based on predicted transcriptional outputs, beginning with MDR1. MDR1-dependent Rh123 efflux was undetectable in circulating naïve $CD4^+$ and Treg cells, consistent with our prior studies[27], but increased progressively as human Teff cells acquired expression of α4 integrin, β7 integrin, and CCR9 (**Fig. 4d-e**). $\alpha4^+\beta7^+CCR9^+$ Teff cells were enriched for the $CCR6^+CXCR3^{hi}CCR4^{lo}$ "Th17.1" phenotype, which display both Th17 and Th1 effector functions[33], as well as preferential MDR1 expression[34] (Extended Data Fig. 11a-d). However, combined expression of α4 integrin, β7 integrin, and CCR9 increased the proportion of MDR1-expressing Th17.1 cells, as well as conventional Th17 ($CCR6^+CXCR3^{lo}CCR4^{hi}$) and Th1 ($CCR6^-CXCR3^{hi}CCR4^{lo}$) cells, when compared with lineage counterparts lacking one or more of these small bowel-homing receptors (Extended Data Fig. 11e-f). $\alpha4^+\beta7^+CCR9^+$ Teff cells also displayed increased *ABCB1* mRNA expression, as judged by qPCR, as well as of CAR (*NR1I3*) and *CYP2B6*—the human ortholog of mouse *Cyp2b10*—compared to either naïve, Treg or $\alpha4^-\beta7^-CCR9^-$ Teff cells

(**Fig. 4f**). *IL10* expression was similarly increased in $\alpha4^{+}\beta7^{+}CCR9^{+}$ Teff cells, compared with either naïve T cells or Teff cells lacking small bowel-homing receptors, although this was not as high as the levels of *IL10* seen in Treg cells (**Fig. 4f**). Most importantly, only $\alpha4\beta7^{+}CCR9^{+}$ Teff cells responded to *ex vivo* treatment with the human CAR agonist, 6-(4-Chlorophenyl)imidazo[2,1-b][1,3]thiazole-5-carbaldehyde O-(3,4-dichlorobenzyl) oxime (CITCO)[35] by upregulating *CYP2B6* expression (**Fig. 4g**). These data suggest that CAR is also expressed in human Teff cells, where its transcriptional activity appears to be tied to small bowel-homing activity.

BAs have emerged as important and pleotropic signaling metabolites that can have both pro- and anti-inflammatory effects in the gastrointestinal tract via dynamic interactions with both germline-encoded host receptors and the microbiota[36-40]. Our study suggests a novel function of the BA- and xenobiotic-sensing nuclear receptor, CAR, in mucosal T cells. Based on both gene expression and functional studies, we propose that CAR initiates a dedicated and diverse program of gene expression in siLP Teff cells to prevent BA toxicity and maintain small bowel immune homeostasis. Pharmacologic CAR activation may offer an unexpected strategy for treating small bowel Crohn's disease, and provides new insight into the specialization of lymphocytes in discrete non-lymphoid tissues.

EXPERIMENTAL PROCEDURES

Mice

Wild type C57BL/6, B6.CD45.1^{+}, B6.*Rag1*$^{-/-}$ and B6.*Rag2*$^{-/-}$ mice were purchased from The Jackson Laboratory. Wild type FVB/N mice were purchased from Taconic. B6.*Nr1i2*$^{-/-}$, B6.*Nr1i3*$^{-/-}$ and B6.*Nri12*$^{-/-}$ *Nr1i3*$^{-/-}$ mice were generated in the Moore lab. FVB.*Rag1*$^{-/-}$ mice were a gift of Dr. Allan Bieber (Mayo Clinic, Rochester, MN). B6 Rag1-deficient mice lacking the Asbt transporter (*Rag1*$^{-/-}$*Slc10a2*$^{-/-}$) were generated as previously described[4]. Lumen contents were collected from conventionally-housed or germ-free wild type B6 mice housed at the Weaver lab at the University of Alabama-Birmingham (UAB). All breeding and experimental use of animals was conducted in accordance with protocols approved by The Scripps Research Institute (TSRI) Florida, Baylor College of Medicine (BCM) or UAB IACUC committees.

Human blood samples

Human blood samples were collected and analyzed in accordance with protocols approved by Institutional Review Boards at TSRI, OneBlood (Orlando, Florida), and The University of Miami. Blood was obtained after informed written consent, and consenting volunteers willingly shared clinical history and demographic data prior to phlebotomy. Institutional Review Boards at OneBlood and The University of Miami approved all procedures and forms used in obtaining informed consent, and all documentation for consenting volunteers is

stored at OneBlood. Cryopreserved PBMC samples were stored in de-identified vials and shipped to TSRI Florida for analyses.

$CD4^+$ T cell isolation and culture

Purified $CD4^+CD25^-$ T cells were magnetically isolated from mononuclear cells from spleen and peripheral lymph nodes using an EasySep magnetic T cell negative isolation kit (Stem Cell Technologies, Inc.) and included a separate additional biotin anti-mouse CD25 antibody (0.5 μg/mL; eBioscience). Magnetically-enriched $CD4^+$ T cells were cultured in Dulbecco's modified Eagle's medium (DMEM) supplemented with 10% heat-inactivated fetal bovine serum, 2mM L-glutamine, 50uM 2-mercaptoethanol, 1% MEM vitamin solution, 1% MEM non-essential amino acids solution, 1% Sodium Pyruvate, 1% Arg/Asp/Folic acid, 1% HEPES, 0.1% gentamicin and 100u/ml Pen-Strep. For *Rag1*$^{-/-}$ transfer experiments, purified $CD4^+CD25^-$ T cells were further FACS-sorted to obtain pure naïve T cells ($CD3^+CD4^+CD25^-CD62L^{hi}CD44^{lo}$). For *in vitro* $CD4^+$ T cell activation, tissue-culture plates were coated for 1-2 hr at 37 ^oC with goat-anti-hamster whole IgG (0.3 mg/mL) and washed with PBS. Purified $CD4^+$ T cells were activated at $4x10^5$ cells/cm^2 and $1x10^6$ cells/mL in 96 and 24 well flat bottom plates coated with hamster-anti-mouse CD3ε (0.3 μg/mL) CD28 (0.5 μg/mL). At 48 hr post-activation, cells were removed from TCR stimulation and re-cultured at $1x10^6$ cells/mL in 10 U/mL recombinant human IL-2 (rhIL-2) (NIH Biorepository).

Retroviral plasmids and transductions

shRNAmirs against mouse nuclear receptors were purchased (TransOMIC) or custom synthesized using the shERWOOD algorithm[41]. For cloning into an ametrine-expressing murine retroviral vector (LMPd) containing the enhanced miR-30 cassette[42,43], shRNAmirs were PCR amplified using forward (5′-AGAAGGCTCGAGAAGGTATATTGC-3′) and reverse (5′-GCTCGAATTCTAGCCCCTTGAAGTC CGAGG-3′) primers containing XhoI and EcoR1 restriction sites, respectively. All retroviral constructs were confirmed by sequencing prior to use in cell culture experiments. Retroviral particles were produced by transfection of Platinum E (PLAT-E) cells with the TransIT-LT1 transfection reagent (Mirus) in Opti-MEM I reduced serum medium. Viral supernatants containing 10 μg/mL polybrene were used to transduce $CD4^+CD25^-$ T cells 24 hr post stimulation, centrifuged 2000 rpm for 1 hour at room temperature and incubated at 37 ^oC until 48 hr post activation and expanded in complete media containing 10 U/mL rhIL-2.

Cell lines

PLAT-E cells, derived from the HEK-293 human embryonic kidney fibroblasts and engineered for improved retroviral packaging efficiency, were provided by Dr. Matthew Pipkin (TSRI Florida). All cell lines were tested

to be mycoplasma free, and cultured in DMEM plus 10% FBS, 2 mM L-glutamine, 50 uM 2-mercaptoethanol, 1% HEPES, 0.1% gentamicin and 100u/ml Pen-Strep.

T Cell transfer model of colitis

For T cell transfer experiments using wild-type B6 or B6.*Nr1i3*$^{-/-}$ T cells, 0.5 x 10^6 FACS-sorted naïve T cells (sorted as $CD4^+CD25^-CD62L^{hi}CD44^{lo}$ at TSRI Florida; $CD4^+CD45RB^{hi}$ at BCM) were injected intraperitoneally (i.p.) into syngeneic B6.*Rag1*$^{-/-}$, B6.*Rag2*$^{-/-}$, or B6.*Rag1*$^{-/-}$*Asbt*$^{-/-}$ recipients and analyzed between 2-6 weeks post-transfer. For congenic T cell transfer experiments, FACS-purified naïve T cells ($CD4^+CD25^-CD62L^{hi}CD44^{lo}$) from B6.CD45.1$^+$, B6.*Nr1i2*$^{-/-}$, B6.*Nr1i3*$^{-/-}$, or B6.*Nri12*$^{-/-}$*Nr1i3*$^{-/-}$ mice were mixed in a 1:1: ratio and 0.5 x 10^6 cells were co-adoptively transferred into syngeneic B6.*Rag1*$^{-/-}$ recipients and analyzed on week 6 after transfer. For transfers of shRNAmir-expressing T cells, magnetically isolated FVB wild-type naïve T cells were activated *in vitro* using plate-bound anti-CD3/anti-CD28 antibodies, transduced 24 hr post-activation with shRNAmir-expressing retroviruses, and expanded until day 5 in media supplemented with rhIL-2 and transduced T cells were FACS-sorted on live (viability dye$^-$) ametrine$^+$ cells prior to transfer and analyzed on week 6. In some experiments, 0.5 x 10^6 unsorted T cells, containing both transduced and untransduced T cells, were transferred into syngeneic FVB.*Rag1*$^{-/-}$ mice. All *Rag1*$^{-/-}$ recipients were weighed immediately prior to T cell transfer to determine baseline weight, and then weighed twice weekly after T cell transfers for the duration of the experiment. Mouse chow diets containing 2% Cholestyramine (CME) (Sigma) or 0.2% Cholic Acid (CA) (Sigma) and control diets were custom made (Teklad Envigo, Madison, WI) and used for mouse feeding as indicated below: cholestyramine diet was started at 3 weeks post-T cell transfer and continued for 3 weeks; cholic acid diet was started within 3 days post-T cell transfer and continued for 6 weeks (or until mice died). TCPOBOP (TC; Sigma-Aldrich) was initially reconstituted in sterile DMSO, stored at -20 ^oC, and diluted in sterile saline and sonicated immediately prior to injections. 3 mg/kg TC was injected intra-peritoneal (i.p.) weekly as indicated. Transferred *Rag1*$^{-/-}$ or *Rag2*$^{-/-}$ mice were euthanized upon losing 20% of pre-transfer baseline weight. All *Rag*$^{-/-}$ mice receiving different donor T cell genotypes were co-housed throughout to normalize microflora exposure.

Anti-CD3-induced intestinal injury

Wild-type (B6) or CAR-deficient (B6.*Nr1i3*$^{-/-}$) mice were injected i.p. with 15 ug of soluble, Ultra-LEAF purified anti-CD3 (clone: 145-2C11) or IgG isotype control (clone: HTK888) (BioLegend) twice over 48 hr. Animals were euthanized, and T cells analyzed 4 hr after the second injection.

Histology

Colon (proximal, distal) or small intestine (proximal, mid, distal/ileum) sections (~ 1 cm) were cut from euthanized *Rag1*$^{-/-}$ or *Rag2*$^{-/-}$ mice 6 weeks post-T cell transfer. In some experiments, 10 cm segments of distal small intestine and whole colon were dissected from mice and fixed intact. All tissues were fixed in 10% neutral buffered formalin, embedded into paraffin blocks, cut for slides, and stained with hematoxylin and eosin (H&E). H&E-stained sections were analyzed and scored blindly as in[44].

Mononuclear cell isolation

Mouse single-cell mononuclear suspensions were prepared from spleen, peripheral lymph nodes, or mesenteric lymph nodes (MLN) by mechanical disruption passing through 70 μm nylon filters (BD Biosciences). For isolating cells from intestinal tissues, small intestines and colons were removed, rinsed thoroughly with PBS to remove the fecal contents, and opened longitudinally; Peyer's patches were removed from small intestines. Tissues were incubated for 30 minutes at room temperature in DMEM media without phenol red (Thermo Fisher Scientific) plus 0.15% DTT (Sigma-Aldrich) to eliminate mucus layer. After washing with media, intestines were incubated for 30 minutes at room temperature in media containing 1 mM EDTA (Amresco) to remove the epithelium. Intestinal tissue was digested in media containing 0.25 mg/mL liberase TL and 10 U/mL RNase-free DNaseI for 15-25 minutes at 37 ^{o}C. Lymphocyte fractions were obtained by 70/30% Percoll density gradient centrifugation (Sigma-Aldrich). Mononuclear cells were washed in complete T cell media and resuspended for downstream FACS analysis or sorting.

Flow cytometry

Cell surface and intracellular FACS stains were performed at 4 ^{o}C for 30 minutes, washed with phosphate buffered saline (PBS) and acquired on a flow cytometer. For all intracellular stains, cells were stimulated for 3-4 hr with phorbol 12-myrisate 13-acetate (PMA) and ionomycin in the presence of brefeldin A (BFA) (all from Sigma-Aldrich) prior to antibody staining. Rh123 assay was performed by labeling mononuclear cells with 1 μg/mL Rh123 in complete medium 4 ^{o}C for 30 minutes, washed and incubated with pre-warmed media at 37 ^{o}C for 45 minutes; surface staining was performed afterwards. Background Rh123 efflux was determined by the addition of the MDR1 antagonist, elacridar (10 nM), to Rh123-labelled cells prior to efflux at 37 ^{o}C. Anti-mouse antibodies used for FACS analysis included: Alexa Fluor 700 anti-CD45, APC anti-CD45.1, BV711 anti-CD4, BV510 anti-CD25, BV650 anti-CD3, Percp-Cy5.5 anti-CD62L, PE-CY7 anti-CD44, BV605 anti-CD62L, PE anti-α4β7 (from BioLegend); and BUV395 anti-CD3, PE-CF594 anti-CD25, FITC anti-Ki67, PE-CF594 anti-CD25 (from BD). Anti-human antibodies used for FACS analysis included: APC anti-CD3, PE anti-CD4, PE-Cy7 anti-CD45RO, PE-CF594 anti-CD25 (from BD), BV711 anti-CD49a (integrin α4), APC-Fire 750 anti-integrin β7, BV421 anti-CCR9, and Percp-Cy5.5 anti-CCR7. Vital dyes include: fixable viability eFluor® 506, eFluor® 660 and eFluor® 780 (all from eBioscience). Rh123 and elacridar were purchased from Sigma-

Aldrich. All FACS data was acquired on LSRII or FACSCanto II instruments (BD), and analyzed using FlowJo 9 or FlowJo 10 software (TreeStar, Inc.).

FACS sorting

Surface staining was performed, filtered through 70 μm nylon filters, resuspended in PBS plus 1% serum, and sorted on a FACS AriaII machine (BD Biosciences). Sorted cells were collected in serum-coated tubes containing PBS plus 50% serum. Gates used to sort MDR1+/- T cells established on Rh123 efflux were set based on background Rh123 efflux in elacridar-treated cells. For human T cell sorts, PBMC was isolated using Ficoll-Plaque PLUS (GE Healthcare) from 25 mL of enriched buffy coats (OneBlood). PBMC was enriched using the Human total CD4 T cell Negative Isolation kit, followed by either Human Memory CD4 T cell Enrichment (EasySep) or Human $CD4^{+}CD127^{lo}CD49d^{-}$ Treg Enrichment Kit (StemCell Technologies). Enriched cells were stained with anti-human FACS antibodies (listed above) for 20 minutes on ice. Stained cells were filtered through sterile 50 uM mesh filters and re-suspended in PBS with 5% FBS and 0.1% DNase. In cases where RNA was isolated after sorting, 100,000 cells were sorted into 200 uL PBS with 1 uM DTT and 5 uL RNase Inhibitor Cocktail (Takara); for *ex vivo* culture experiments, 0.4-1.2 $x10^{6}$ cells were sorted into complete T cell media.

Pooled *in vivo* shRNAmir screen

Two independent pooled screens were performed. Briefly, PLAT-E cells were cultured in 96 well plates with 5 x 10^{4} per well in 100uL complete medium and transfected as described above. Magnetically enriched $CD4^{+}CD25^{-}$ T cells from spleens of 7- to 8-week old female FVB/N (FVB) mice were activated with anti-CD3 and anti-CD28 in 96 well plates and transduced 24 hr post-activation. Transduction efficiency of each individual shRNA was determined on day 4; transduced cells were pooled and FACS-sorted for $ametrine^{+}$ on day 5 and adoptively transferred (i. p.) into 10 FVB.*Rag1*$^{-/-}$ mice. An aliquot of sorted cells was saved for genomic DNA isolation and used for input reference. Six weeks post-transfer, live ($viability\ dye^{-}$) transduced ($ametrine^{+}$) $Rh123^{hi}$ ($Mdr1^{-}$) or $Rh123^{lo}$ ($Mdr1^{+}$) effector/memory T cells (Teff; $CD4^{+}CD25^{-}CD62L^{lo}CD44^{hi}$) were FACS-sorted from the spleen or small intestine lamina propria of FVB.*Rag1*$^{-/-}$ recipients. High quality genomic DNA was isolated using PureLink® Genomic DNA Mini Kit (Invitrogen) and 100 ng of DNA was used for library preparation. gDNA derived from transduced and sorted T cells were quantified with Qubit DNA assay. 75ng of gDNA were used as template in duplicate reactions to add the Ion adapter sequences and barcodes. Based on previous data, 28 cycles of PCRs were used to amplify the libraries using primers with Ion P1 miR30 loop sequence (5'-CCTCTCTATGGGCAGTCGGTGATTACATCTGTGGCTTCACTA-3') and Ion A miR-30 (5'-CCATCTCATCCCTGCGTGTCTCCGACTCAGXXXXXXXXXXGCTCGAGAAGGTATATTGCT-3')

sequences. The miR-30 loop (PI) and miR-30 (A) annealing sequences are underlined. The IonXpress 10 nt barcode is depicted with a string of X's. Sequencing libraries were purified with 1.6X Ampure XP beads (Beckman Coulter), quantified with Qubit DNA HS assay (Invitrogen), and visualized on the Agilent 2100 Bioanalyzer (Agilent Technologies, Inc.). Individually-barcoded libraries were pooled at equimolar ratios and templated on to Ion spheres at 50 pM loading concentration using the Ion Chef (Life Technologies) with the Ion PI IC 200 kit (cat. #4488377). The templated Ion spheres (ISPs) were quantified using AlexaFluor sequence-specific probes provided in the Ion Spehere quality control kit (Life Technologies, cat #: 4468656). The percent templated ISPs within 10-20% were taken forward to loading on the Ion PI V2 chips and then run on the Ion Proton with 200 bp reads. Libraries were sequenced using the Ion Torrent technology from Life Technologies following the manufacturer's instructions. Sequencing reads were aligned to the reference library using BLAST with default settings and raw counts were normalized with DESeq2. Normalized reads of shRNAmirs displaying $\leq$ 10-fold change between input and *ex vivo* spleen samples were considered for downstream analysis. The relative enrichment or depletion of shRNAmirs from each population was determined by median $\log_2$ fold-change in abundance of shRNAmirs in $Mdr1^{hi}$ *vs*. $Mdr1^{lo}$ siLP Teff cells.

Modulation of Teff cell gene expression by pharmacological compounds or tissue extracts

For *ex vivo* mouse T cell culture experiments, 30,000 CD45.1 (wild type) or CD45.2 (*Nr1i3*$^{-/-}$) Teff cells FACS-purified from spleens of B6.*Rag1*$^{-/-}$ mice 3-weeks after congenic naïve T cell transfer were activated in round-bottom 96-well plates with mouse anti-CD3/anti-CD28 T cell expander beads (1 bead/cell; ThermoFisher) in complete media containing 10 U/mL recombinant human (rh) IL-2 for 24 hr in the presence or absence of 10 or 20 uM 1,4-Bis-[2-(3,5-dichloropyridyloxy)]benzene, 3,3′,5,5′-Tetrachloro-1,4-bis(pyridyloxy)benzene (TC), 10 uM 5α-Androstan-3β-ol (And), 10 uM 5-Pregnen-3β-ol-20-one-16α-carbonitrile (PCN) (all from Sigma-Aldrich), 1% serum, 0.1% bile (from gallbladder), 1% soluble small intestine lumen content (siLC), or 1% soluble colon lumen content (cLC) isolated from wild type (B6) mice. An equal volume of sterile vehicles (DMSO for TC, And; ethanol for PCN; PBS for sterile mouse content) were used for negative controls. For human T cell culture experiments, healthy adult donor PBMC were FACS-sorted for the following subsets: (*i*) naïve $CD4^+$ T cells ($CD4^+CD25^-CD45RO^-CCR7^{hi}$); (*ii*) Treg cells ($CD4^+CD25^{hi}$); (*iii*) $\alpha4^-CCR9^-$ effector/memory cells (Teff; $CD4^+CD25^-CD45RO^+$); and (*iv*) $\alpha4^+CCR9^+$ effector/memory cells (Teff; $CD4^+CD25^-CD45RO^+$). Note that all $\alpha4^-CCR9^-$ Teff cells are integrin $\beta7^-$and all $\alpha4^+CCR9^+$ Teff cells are integrin $\beta7^+$. For all subsets, 30,000 purified cells were stimulated in round-bottom 96-well plates with human anti-CD3/anti-CD28 T cell expander beads (1 bead/cell; ThermoFisher) in complete media containing 10 U/mL rhIL-2 with or without 10 or 20 uM 6-(4-Chlorophenyl)imidazo[2,1-b][1,3]thiazole-5-carbaldehyde O-(3,4-dichlorobenzyl)oxime (CITCO) (Sigma-Aldrich); an equal volume of DMSO served as the negative control.

qPCR

RNA was isolated from cultured or ex vivo-isolated cells using RNeasy columns with on-column DNase treatment (Qiagen); RNA was used to synthesize cDNA via a high capacity cDNA reverse transcription kit (Life Technologies/Applied Biosystems). Taqman qPCR was performed on a StepOnePlus real time PCR instrument (Life Technologies/Applied Biosystems) using commercial Taqman primer/probe sets (Life Technologies). Probes for mouse genes included: *Abcb1a* (Mm00607939_s1), *Nr1i3* (Mm01283981_g1), *Cyp2b10* (Mm01972453_s1), *Il10* (Mm01288386_m1) and *Actin b (Mm00607939_s1)*; probes for human genes included: *NR1I3* (Hs00901571_m1), *ABCB1* (Hs00184500_m1), *CYP2B6* (Hs04183483), *IL10* (Hs00961622_m1), and *ACTIN B* (Hs0160665_g1).

Bioinformatics analyses

ChIP-seq: Raw sequencing reads for CAR were downloaded from Gene Expression Omnibus (GSE112199)[20], aligned to USC mm10 with Bowtie2[45] and analyzed with MACS[46] using base settings. Biological replicate reads files were merged into a single file and bigwig files were generated and visualized with Integrated Genome Viewer (IGV)[47]. Peaks were filtered to remove reads with alternative annotations, mitochondrial DNA, or blacklist regions in R using GenomeInfoDb and GenomicRanges package.

RNA-seq: Next-generation RNA-sequencing (RNA-seq) was performed on FACS-sorted B6 wild type and CAR-deficient effector/memory T cells (Teff cells: viability dye^{-}CD45^{+}CD3^{+}CD4^{+}CD25^{-}CD44^{hi}) from spleen, small intestinal lamina propria, and colon lamina propria of B6.*Rag1*$^{-/-}$ mice injected 3 weeks prior with congenic mixtures of CD45.1 wild type and CD45.2 *Nr1i3*$^{-/-}$ naïve T cells, approximately 500 sorted cells were processed directly to generate cDNA using the Clontech SMART-Seq v4 Ultra Low Input Kit (Clontech, Inc.) on three biologically-independent replicates. The generated cDNA was size selected using beads to enrich for fragments > 400 bp. The enriched cDNA was converted to Illumina-compatible libraries using the NEBNext Ultra II DNA kit (New England Biolabs, Inc.) using 1ng input. Final libraries were validated on the Agilent 2100 bioanalyzer DNA chips and quantified on the Qubit 2.0 fluorometer (Invitrogen, Life Technologies). Barcoded libraries were pooled at equimolar ratios and sequenced using single-end 75 bp reads on a NextSeq 500 instrument (Illumina). Raw sequencing reads (fastq files) were mapped to the mm10 transcriptome and transcript abundance in terms of Transcripts Per Million (TPM) were quantified using Salmon[48]. PCA was performed and projected in R-studio. Differentially expressed genes (DEG) were determined using DESeq2 ($P < .05$) for CAR-deficient (B6.*Nr1i3*$^{-/-}$) *vs.* wild type (B6) Teff cells from spleen (296 up; 285 down), siLP (472 up; 523 down), or cLP (350 up; 228 down) and $\log_2$ fold-change was used as the ranking metric to generate input ranked lists for gene set enrichment analysis (GSEA) (https://www.gsea-msigdb.org/gsea/index.jsp); these genes were compared against both customized and curated gene sets (the latter from the Molecular Signature Database (MSigDB)) for enrichment—quantified as normalized enrichment score (NES)—and visualized using

ggplot2 package in R. Differentially expressed genes of wild type (B6) Teff cells from the spleen, siLP, or cLP determined by DESeq2 were used to generate tissue-specific Teff gene sets: (*i*) up in B6 spleen Teff, genes selectively expressed in spleen *vs*. either siLP or cLP wild type (B6) Teff cells; (*ii*) up in B6 siLP Teff, genes selectively expressed in siLP *vs*. either spleen or cLP wild type (B6) Teff cells; and (*iii*) up in B6 cLP Teff, genes selectively expressed in cLP *vs*. either spleen or siLP wild type (B6) Teff cells. RNA-seq data of pharmacological activation of CAR or PXR in hepatocytes *in vivo* from mice treated with the CAR agonist, TCPOBOP (TC), the PXR agonist, PCN, or vehicle (corn oil) (GSE104734)[18] were analyzed to generate the gene sets: Up in Hep + TC, genes selectively induced by the CAR agonist, TCPOBOP (TC), compared with either vehicle (corn oil) or the PXR agonist, PCN, in hepatocytes from mice treated with compounds *in vivo*; and Up in Hep + PCN, genes selectively induced by the PXR agonist, PCN, compared with either vehicle (corn oil) or the CAR agonist, TC, in hepatocytes from mice treated with compounds *in vivo*. Differential gene expression of *in vitro*-differentiated Tr1 (GSE92940)[21] and Th17 cells (GSE21670)[24] were determined using the Limma package in R (for microarray data)[49] to generate the gene sets: Tr1-signature, genes selectively expressed in *in vitro*-differentiated Tr1 cells, compared with non-polarizing conditions; and Th17-signature, genes selectively expressed in *in vitro*-differentiated Th17 cells, compared with non-polarizing conditions. Th1-signature, Th2-signature, induced (i)Treg-signature (GSE14308)[50], or T follicular helper (Tfh)-signature (GSE21379)[51], genes selectively induced in these *vs*. other T cell subsets, as curated on MSigDB (https://www.gsea-msigdb.org/gsea/msigdb/index.jsp).

TR-FRET co-regulator recruitment assay

The DNA sequences encoding mouse (m)CAR ligand-binding domain (LBD; residues 109 – 358) were amplified by PCR reaction and inserted into modified pET24b vectors to produce pET24b-mCAR-LBD. pACYC-Duet1-RXR-LBD, an expression plasmid for untagged human (h)RXRα LBD was provided by Dr. Eric Xu[52]. Purification of the mCAR-hRXR LBD heterodimer, as well as hRXR homodimer, was achieved by nickel-affinity chromatography, followed by size-exclusion chromatography in an Akta explorer FPLC (GE Healthcare). Briefly, pET24b-mCAR-LBD and pACYC-Duet1-RXR-LBD were co-transformed into BL21 (DE3) for mCAR-hRXR heterodimer and pET46-RXR-LBD was transformed into BL21 (DE3) for RXR homodimer. The cells were grown in 4 x 900 mL of LB media at 37 °C until the OD600 reached a value of 0.6–0.7. Overexpression was induced by 0.3 mM of IPTG and the cells were grown further for 22 hr at 18 °C. The harvested cells were resuspended in sonication buffer (500 mM NaCl, 10 mM HEPES, 10 mM imidazole, pH 8.0, and 10% glycerol), sonicated on an ice-water bath for 20 min at 18 W output, and centrifuged for 25 min at 50,000 x g. The proteins were isolated from the sonicated supernatant by applying to a 2 mL His Select column and eluted with linear gradient from 10 mM to 300 mM imidazole in sonication buffer. The elution fractions containing the proteins concentrated while exchanging buffer to gel filtration buffer (300 mM NaCl, 20 mM

HEPES, 1 mM DTT, 5 % glycerol). The proteins were purified further by gel filtrations through a Superdex 200 26/60 column (GE Healthcare) equilibrated with gel filtration buffer. Fractions containing the proteins were pooled and concentrated to ~ 8 mg/mL each with 30 kDa cutoff ultrafiltration units (Millipore). For preparation of mouse content, mouse small intestinal lumen content (siLC) or colon lumen content (cLC) was extracted from whole tissue into a sterile tube. Contents were weighed, diluted with an equal volume of sterile PBS, vortexed vigorously for 30 sec, and then supernatants were collected after sequential centrifugation steps: (*i*) 10 min at 930 x *g*; and (*ii*) 10 min at 16 x *g*. Cleared supernatants were finally sterile-filtered using 0.22 μm filters and aliquots were frozen at -20^{o} C. Serum was collected in EDTA coated tubes and centrifuged for 5 min at 2.4 x *g*. Due to small sample size, serum and gallbladder bile were used directly without filter sterilization after harvesting. Time-resolved fluorescence resonance energy transfer (TR-FRET) assays were performed in low-volume black 384-well plates (Greiner) using 23 μL final well volume. Each well contained the following components in TR-FRET buffer (20 mM KH_2PO_4/K_2HPO_4, pH 8, 50 mM KCl, 5 mM TCEP, 0.005% Tween 20): 4 nM 6xHis-CAR/RXRα LBD heterodimer or 6xHis-RXRα/RXRα homodimer LBD, 1 nM LanthaScreen Elite Tb-anti-His Antibody (ThermoFisher #PV5895), and 400 nM FITC-labeled PGC1α peptide (residues 137–155, EAEEPSLLKKLLLAPANTQ, containing an N-terminal FITC label with a six-carbon linker, synthesized by Lifetein). Pure ligand (TC) or metabolic extracts were prepared via serial dilution in vehicle (DMSO or PBS, respectively), and added to the wells along with vehicle control. Plates were incubated at 25 °C for 1 hr and fluorescence was measured using a BioTek Synergy Neo plate reader (Promega). The terbium (Tb) donor was excited at 340 nm, its emission was monitored at 495 nm, and emission of the FITC acceptor was monitored at 520 nm. Data were plotted as 520/340 nM rations using Prism software (GraphPad); TC data were fit to a sigmoidal dose response curve equation.

Quantification and Statistical Analyses

Statistical analyses were performed using Prism (GraphPad). *P* values were determined by paired or unpaired student's *t* tests, Log-rank test, one-way ANOVA, and two-way ANOVA analyses as appropriate and as listed throughout the Figure legends. Statistical significance of differences (* $P < 0.05$, ** $P < 0.01$, *** $P < 0.001$, **** $P < 0.0001$) are specified throughout the Figure legends. Unless otherwise noted in legends, data are shown as mean values ± S.E.M. For histological analyses, trained veterinary pathologists were 'blinded' to the allocation of animals and experimental groups.

FIGURE LEGENDS

Fig. 1. A pooled *in vivo* RNAi screen identifies CAR as a transcriptional regulator of MDR1 expression in mucosal T cells. (a) Naïve CD4^{+} T cells (Tnaive), from spleens of FVB/N (FVB) wild type mice, were

activated with anti-CD3/anti-CD28 antibodies in 96-well plates and transduced 24 hr post-activation with retroviral supernatants produced in PLAT-E packaging cells, one shRNAmir clone per well. Transduced cells were expanded in IL-2-containing media until day 5, after which cells were pooled, FACS-sorted for transduced (ametrine^{+}) cells and transferred into 10 FVB.*Rag1*$^{-/-}$ recipient mice; an aliquot of the pooled and sorted "input" cells was frozen for subsequent genomic (g)DNA isolation and next-generation sequencing (DNA-seq). Live (viability dye^{-}) transduced (ametrine^{+}) effector/memory (Teff; CD4^{+}CD25^{-}CD62L^{lo}CD44^{hi}) cells were re-isolated by FACS-sorting 6-weeks post-T cell transfer from spleen or small intestine lamina propria (siLP). Total transduced spleen Teff cells were collected, and both spleen and siLP Teff cells were further sub-divided into Mdr1^{hi} and Mdr1^{lo} subsets, based on efflux of the Mdr1 fluorescent substrate, Rh123. gDNA from all 6 Teff cell pools were subjected to DNA-seq to quantify shRNAmir abundance. **(b)** *Top*, abundance of shRNAmirs in *ex vivo*-isolated spleen and *in vitro*-transduced (input) Teff cells. shRNAmirs with $\leq$ 1 normalized read in both *ex vivo* spleen and input Teff cell pools were considered 'poorly represented' (highlighted green). Well-represented shRNAmirs displaying $\leq$ 10-fold change between *ex vivo* spleen and input Teff cell pools (between blue lines) were considered for downstream analysis. *Bottom*, abundance of shRNAmirs, filtered for minimal effects on *in vivo* Teff cell persistence, in *ex vivo*-isolated Mdr1^{hi} (Rh123^{lo}) and Mdr1^{lo} (Rh123^{hi}) siLP Teff cells. **(c)** Median $\log_2$ fold-change in abundance of shRNAmirs in Mdr1^{hi} *vs.* Mdr1^{lo} siLP Teff cells as in (b). Dashed horizontal lines indicate 2-fold changes. (a-c) Data incorporates shRNAmir abundance, determined by DNA-seq, in 2-indpeendent screens using pooled spleens and siLP from 10 transferred FVB.*Rag1*$^{-/-}$ mice per screen. **(d)** Diagram of the *Nr1i3*/CAR locus. Seed sequence positions for each of the 5 shRNAmirs targeting CAR (*shNr1i3s*) are shown; 5' and 3' untranslated regions (UTR) are indicated; exons are denoted by filled boxes. **(e)** *Left*, mean weight loss ($\pm$ SEM; n = 46) in co-housed FVB.*Rag1*$^{-/-}$ mice injected with FVB wild type CD4^{+} T cells transduced *in vitro* with a negative control shRNAmir against CD8 (*shCd8a*; n = 11), or the indicated shRNAmirs against CAR (*shNr1i3*s); *shNr1i3.1* (n = 7), *shNr1i3.2* (n = 7), *shNr1i3.3* (n = 7), *shNr1i3.4* (n = 7), *shNr1i3.5* (n = 7). *** P < .001, **** P < .0001, Two-way ANOVA. *Right*, correlation between mean weight loss induced by Teff cells in FVB.*Rag1*$^{-/-}$ recipients (at 6-weeks post-T cell transfer) and mean percent of Mdr1-dependent Rh123 efflux in *ex vivo*-isolated spleen Teff cells (determined by flow cytometry as in Extended Data Fig. 2b-c). ** P < .01, Pearson (r) correlation test. **(f)** *Left*, naïve CD4^{+} T cells from spleens of C57BL/6 wild type (B6; blue) or CAR-deficient (B6.*Nr1i3*$^{-/-}$; red) mice were transferred into separate groups of co-housed B6.*Rag2*$^{-/-}$ recipients. *Middle*, survival in co-housed B6.*Rag2*$^{-/-}$ mice injected with wild-type (B6; n = 7) or CAR-deficient (B6.*Nr1i3*$^{-/-}$; n = 19) naïve CD4^{+} T cells. * P < .05, Log-rank test. *Right*, mean weight loss ($\pm$ SEM; n = 16) in B6.*Rag2*$^{-/-}$ mice transplanted with wild-type (B6; n = 7) or CAR-deficient (B6.*Nr1i3*$^{-/-}$; n = 9) naïve CD4^{+} T cells as in survival. ** P < .01, Two-way ANOVA. **(g)** *Top*, H&E-stained sections of colons or terminal ilea from co-housed B6.*Rag2*$^{-/-}$ mice 6-weeks after transfer of wild-type (B6) or CAR-deficient (B6.*Nr1i3*$^{-/-}$) naïve CD4^{+} T cells as

in (f). Representative of 7 mice per group from two independent experiments. *Bottom*, mean histology scores (± SEM; $n = 7$) for colons or terminal ilea from co-housed B6.*Rag2*$^{-/-}$ mice injected with wild-type (B6) or CAR-deficient (B6.*Nr1i3*$^{-/-}$) naïve CD4^{+} T cells. ** $P < .01$, paired two-tailed student's *t* test.

Fig. 2. CAR preferentially regulates T cell function and inflammation in the small intestine. (a) Equal numbers of CD45.1 wild type (B6; blue) and CD45.2 CAR-deficient (B6.*Nr1i3*$^{-/-}$; red) naïve CD4^{+} T cells were transferred together into B6.*Rag1*$^{-/-}$ mice. Resulting effector T (Teff) cells were FACS-purified 3-weeks later from spleen, small intestine lamina propria (siLP), or colon lamina propria (cLP) and transcriptional profiles were assessed by RNA-seq. **(b)** Principle component analysis (PCA) of gene expression in *ex vivo*-isolated wild type (B6; blue) or CAR-deficient (B6.*Nr1i3*$^{-/-}$; red) Teff cells from spleen, siLP, or cLP of congenically co-transferred B6.*Rag1*$^{-/-}$ mice as in (a). **(c)** Volcano plots showing differentially expressed genes, determined by DEseq2, between either wild type (B6) Teff cells from different tissues (*top*), or CAR-deficient (B6.*Nr1i3*$^{-/-}$) *vs*. wild type (B6) Teff cells from the same tissue (*bottom*). Numbers of genes increased (Up, red) or decreased (Down, blue) are highlighted for each comparison. **(d)** Gene set enrichment analysis (GSEA) summary showing enrichment of gene sets (x-axis) within genes differentially expressed between CAR-deficient (B6.*Nr1i3*$^{-/-}$) and wild type (B6) Teff cells from spleen, siLP or cLP (y-axis). Circle size increases proportionately with -$\log_{10}$ adjusted *P* (Padj) values, and thus reflects significance of enrichment. Circle color represents the directionality of enrichment, based on normalized enrichment score (NES); gene sets enriched among genes expressed higher or lower in CAR-deficient *vs*. wild type Teff cells are colored red or blue, respectively. Gene sets (left to right on x-axis) used for GSEA include: (1) Up in B6 spleen Teff, genes selectively expressed in spleen *vs*. either siLP or cLP wild type (B6) Teff cells, as in (c) and Extended Data Fig. 5a; (2) Up in B6 siLP Teff, genes selectively expressed in siLP *vs*. either spleen or cLP wild type (B6) Teff cells, as in (c) and Extended Data Fig. 5a; (3) Up in B6 cLP Teff, genes selectively expressed in cLP *vs*. either spleen or siLP wild type (B6) Teff cells, as in (c) and Extended Data Fig. 5a; (4) Up in Hep + TC, genes selectively induced by the CAR agonist, TCPOBOP (TC), compared with either vehicle (corn oil) or the PXR agonist, PCN, in hepatocytes from mice treated with compounds *in vivo*[18], as in Extended Data Fig. 5b-c; (5) Up in Hep + PCN, genes selectively induced by the PXR agonist, PCN, compared with either vehicle (corn oil) or the CAR agonist, TC, in hepatocytes from mice treated with compounds *in vivo*[18], as in Extended Data Fig. 5b-c; (6) Tr1-signature, genes selectively expressed in *in vitro*-differentiated Tr1 cells, compared with non-polarizing conditions[21]; (7) Th17-signature, genes selectively expressed in *in vitro*-differentiated Th17 cells, compared with non-polarizing conditions[24]; (8-11) Th1-, Th2-, T follicular helper (Tfh)-, or induced (i)Treg-signature, genes selectively induced in these *vs*. other T cell subsets downloaded from the Broad Institute's Molecular Signature Database (https://www.gsea-msigdb.org/gsea/msigdb/index.jsp). (b-d) Mean normalized gene expression values, expressed as TPM, are shown from 3-independent experiments using Teff cells purified from pooled tissues of

5 congenically co-transferred B6.*Rag1*$^{-/-}$ mice per experiment. **(e)** Intracellular IL-10 and IFNγ expression in wild type (B6) or CAR-deficient (B6.*Nr1i3*$^{-/-}$) RORγt^{-}IL-17A^{-} Teff cells from the indicated tissues of congenically co-transferred B6.*Rag1*$^{-/-}$ mice after 2 weeks (gated as in Extended Data Fig. 6a); representative of 5 mice. Numbers indicate percentages. **(f)** Mean percentages (*left*) or numbers (*right*) (± SEM; *n* = 5) of IL-10-expressing wild type (B6; blue) or CAR-deficient (B6.*Nr1i3*$^{-/-}$; red) Teff cells from tissues of congenically co-transferred B6.*Rag1*$^{-/-}$ mice at 2 weeks, determined by flow cytometry as in (e). * $P < .05$, paired two-tailed student's *t* test. **(g)** Mean relative expression (± SEM; *n* = 3) of *Abcb1a*, *Cyp2b10*, or *Il10*, determined by qPCR, in wild type (B6; blue) or CAR-deficient (B6. *Nr1i3*$^{-/-}$; red) Teff cells isolated from spleens of congenically co-transferred B6.*Rag1*$^{-/-}$ mice 72 hr after a single dose of either the CAR agonist, TCPOBOP (TC), or vehicle. Data are shown as relative expression in Teff cells from TC- *vs*. vehicle-treated mice; individual data points reflect 3-independent TC treatment experiments in which wild type or CAR-deficient Teff cells were isolated from a pool of 5 spleens isolated from identically treated animals. * $P < .05$, paired two-tailed student's *t* test. **(h)** Mean weight loss (± SEM; *n* = 61) of co-housed B6.*Rag2*$^{-/-}$ mice transplanted with wild-type CD4^{+} naïve T cells and maintained on a CA-supplemented diet with (red; *n* = 18) or without TC treatment (blue; *n* = 16), control diet chow with vehicle treatment (black, n = 17) or un-transferred mice fed CA-supplemented diet with vehicle treatment (grey; *n* =10). Weights are shown relative to 3-weeks post-transfer when TC treatments were initiated. * $P < .05$, ** $P < .01$, Two-way ANOVA. **(i)** H&E-stained sections of terminal ilea or colons from B6.*Rag2*$^{-/-}$ mice reconstituted with wild type T cells and treated as above and as indicated. Representative of 3 to 4 mice/group. **(j)** Mean histology scores (± SEM; *n* = 3 to 4) for colons or terminal ilea as in (i). * $P < .05$, one-way ANOVA with Tukey's correction for multiple comparisons. NS, not significant.

Fig. 3. Bile-derived intestinal metabolites activate CAR. **(a)** Recombinant His-tagged mouse CAR ligand-binding domain (LBD) was co-purified from bacteria together with the LBD of human RXRα. His-tagged RXRα LBD homodimers were also purified to serve as specificity controls for CAR activation. CAR:RXR heterodimers (or RXR:RXR homodimers) were used in time-resolved fluorescence resonance energy transfer (TR-FRET) assays, in which excitation of a terbium (Tb)-conjugated anti-His antibody emits fluorescence at 495 nm that overlaps with the excitation wavelength of FITC-conjugated PGC1α co-activator peptide recruitment, which has an emission wavelength of 520 nm. Presence of a CAR agonist ligand (*e.g.*, TCPOBOP (TC); *bottom right* insert) increases FITC-PGC1α peptide recruitment resulting in increased FRET between donor (Tb) and acceptor (FITC) fluorophores. Thus, CAR (or RXR) LBD activation is read out as an increase in the ratio of FITC (520 nm) to Tb (495 nm) fluorescence. The EC_{50} for TC in this assay is ~ 34 nm, consistent with the reported binding-affinity of TC for CAR LBD. **(b)** Mean TR-FRET signals (± SEM; *n* = 3) from CAR:RXR heterodimers (*left*) or RXR:RXR homodimers (*right*) in the presence of titrating concentrations of wild type (B6) mouse small intestine lumen content (siLC), bile (from gallbladder), colon lumen content (cLC),

or serum. The 4 bars for each tissue extract are *(left to right)*: (1) diluent (PBS) alone; (2) 0.01%, (3) 0.1%, and (4) 1%. Values reflect means of 3-independent experiments using extracts from different wild type mice; each concentration from each individual mouse was run in triplicate. * $P < .05$, **** $P < .0001$, one-way ANOVA with Tukey's correction for multiple comparisons. NS, not significant. **(c)** Mean relative expression (± SEM; $n = 3$) of *Abcb1a*, *Cyp2b10*, or *Il10*, determined by qPCR, in wild type (B6) or CAR-deficient (B6.*Nr1i3*$^{-/-}$) Teff cells isolated from spleens of congenically co-transferred B6.*Rag1*$^{-/-}$ mice (as in Extended Data Fig. 9d) and stimulated *ex vivo* with anti-CD3/anti-CD28 antibodies (for 24 hr) in the presence or absence of tissue extracts isolated from wild type (B6) mice as in (b). * $P < .05$, ** $P < .01$, *** $P < .001$, One-way ANOVA with Tukey's correction for multiple comparison. NS, not significant. **(d)** Mean TR-FRET signals (± SEM; $n = 3$) from CAR:RXR heterodimers in the presence of titrating concentrations of siLC isolated from conventionally-housed (Conv) or germ-free (GF) wild type (B6) mice pre-treated with or without cholestyramine (CME) to deplete free bile acids. *** $P < .001$, **** $P < .0001$, One-way ANOVA with Tukey's correction for multiple comparison.

Fig. 4. CAR selectively regulates gene expression in human effector/memory T cells expressing small bowel homing receptors. (a) FACS-based identification of human CD4$^+$ T cell subsets in PBMC from healthy adult human donors. Expression of integrin α4 (α4 int.) in gated naïve (gray), T regulatory (Treg; blue), or effector/memory (Teff; red) T cells is shown at right. **(b)** Expression of integrin β7 (β7 int.) and CCR9 in total naïve CD4$^+$ T cells, or in α4 int.+/- Treg or Teff subsets (gated as in (a)). Representative of 13-independent experiments using PBMC from different donors. **(c)** Percentages (%) of α4$^+$β7$^+$CCR9$^+$ Tnaive, Treg, or Teff cells, determined by flow cytometry as in (a-b). Individual data points for the 13 independent experiments are shown and connected by red lines. ** $P < .01$, One-way ANOVA with Tukey's correction for multiple comparisons. **(d)** *Ex vivo* Rh123 efflux in CD4$^+$ T cell subsets (gated as in a-b) in the presence (gray) or absence (red) of the selective MDR1 inhibitor, elacridar. Representative of 8 experiments. **(e)** Mean percentages (± SEM; $n = 8$) of Rh123^{lo} (MDR1$^+$) Teff subsets, determined by flow cytometry as in (d). **(f)** Mean (± SEM) *ex vivo* expression, determined by qPCR, of MDR1/*ABCB1* ($n = 12$), CAR/*NR1I3* ($n = 12$), *CYP2B6* ($n = 11$), or *IL10* expression ($n = 9$), in FACS-purified α4$^-$β7$^-$CCR9$^-$ or α4$^+$β7$^+$CCR9$^+$ Tnaive, Treg or Teff cells. (e-f) * $P <$ .05, ** $P < .01$, *** $P < .001$, One-way ANOVA with Tukey's correction for multiple comparisons. NS, not significant. **(g)** Mean relative *CYP2B6* expression (± SEM; $n = 5$), determined by qPCR, in CD4$^+$ T cell subsets (as in (f)) activated *ex vivo* anti-CD3/anti-CD28 antibodies in the presence or absence of 10 or 20 μM CITCO for 24 hr. *** $P < .001$, Two-way ANOVA.

EXTENDED DATA FIGURE LEGENDS

Extended Data Figure 1. Construction of a nuclear receptor-focused shRNAmir library. Sequence alignment of 256 of the 258 shRNAmirs used in the pooled *in vivo* RNAi screen. *2 of the 5 shEomes constructs had a 1-bp insertion in the passenger strand; these were used in the screen, but are not aligned and assumed to be inactive. $One shRNAmir against *Prdm1* (Blimp-1) was originally annotated as a negative control shRNAmir against *Cd8a*, but was kept in the final library. Numbering and consensus sequence of the enhanced mir-30 cassette (MirE) is indicated at bottom; location of the 5' and 3' MirE backbone, as well as the conserved loop and variable passenger and guide strands are represented at top.

Extended Data Figure 2. shRNAmir-mediated depletion of select nuclear receptor pathways regulates effector T cell persistence or MDR1 expression *in vivo*. (a) Log_2 fold-change in abundance (± SEM) of shRNAmirs against *Cd19* (*n* = 3), *Abcb1a* (*n* = 2), *Nr1i3* (*n* = 5), *Thra* (*n* = 6), and *Esrra* (*n* = 3) in FVB wild type $Rh123^{lo}$ ($MDR1^{hi}$) *vs*. $Rh123^{hi}$ ($MDR1^{lo}$) effector/memory T cells (Teff; sorted as in Fig. 1a) recovered from spleens or small intestine lamina propria (siLP) of transferred FVB.*Rag1*$^{-/-}$ mice. **(b)** *Ex vivo* Rh123 efflux, determined by flow cytometry, in FVB wild type Teff cells (gated as in Extended Data Fig. 9d) expressing a control shRNAmir against CD8 (*shCD8a*) or 1 of 5-independent shRNAmirs against CAR (*shNr1i3*) isolated from spleens of transferred FVB.*Rag1*$^{-/-}$ mice 6-weeks post-transfer. Rh123 efflux in transduced (Ametrine pos.; blue) cells is overlaid with that in congenically-transferred untransduced (Ametrine neg.; red) Teff cells from the same mouse. Background Rh123 efflux in untransduced Teff cells treated with the MDR1 inhibitor, elacridar, is shown in gray. Representative of 63 mice analyzed over 3-independent experiments. **(c)** Mean normalized *ex vivo* Rh123 efflux (± SEM; *n* = 63) in FVB wild type spleen Teff cells expressing control (*shCd8a*; *n* = 11) or CAR-targeting (shNr1i3) shRNAmirs; *shNr1i3.1* (*n* = 10), *shNr1i3.2* (*n* = 10), *shNr1i3.3* (*n* = 12), *shNr1i3.4* (*n* = 10), *shNr1i3.5* (*n* = 10), determined by flow cytometry as in (b). Rh123 efflux was normalized to control *shCd8a*-expressing Teff cells after calculating the change (Δ) in Rh123 mean fluorescence intensity (MFI) between congenically-transferred transduced (ametrine pos.) *vs*. untransduced (ametrine neg.) Teff cells. * $P < .05$, **** $P < .0001$, One-way ANOVA with Tukey's correction for multiple comparisons. **(d)** Mean relative *Abcb1a*, *Nr1i3*, and *Cyp2b10* expression (± SEM), determined by qPCR, in FVB spleen Teff cells FACS-sorted from FVB.*Rag1*$^{-/-}$ recipient mice expressing either a negative control shRNAmir against CD8 (*shCd8a*; *n* = 11), or the indicated shRNAmirs against CAR (*shNr1i3*s); *shNr1i3.1* (*n* = 7), *shNr1i3.2* (*n* = 7), *shNr1i3.3* (*n* = 7), *shNr1i3.4* (*n* = 7), *shNr1i3.5* (*n* = 7).* $P < .05$, ** $P < .01$, *** $P < .001$, **** $P < .0001$, One-way ANOVA with Tukey's correction for multiple comparison. **(e)** Median log_2 fold change in shRNAmir abundance between FVB wild type *ex vivo*-isolated spleen *vs*. *in vitro*-transduced (input) Teff cells. (a, d) shRNAmir abundance reflects the mean number of normalized reads, by DNA-seq, in the indicated Teff subsets obtained in 2-independent screens, each using cells transferred into 10 FVB.*Rag1*$^{-/-}$ mice.

Extended Data Figure 3. CAR, but not PXR, regulates MDR1 expression in effector T cells *in vivo*. (a) *Left*, *ex vivo* Rh123 efflux, determined by flow cytometry, in CD45.1 wild type (B6; red) or CD45.2 CAR-deficient (B6.*Nr1i3*$^{-/-}$), PXR-deficient (B6.*Nr1i2*$^{-/-}$) or CAR/PXR double-deficient (B6.*Nr1i3*$^{-/-}$*Nr1i2*$^{-/-}$) effector/memory T cells (Teff; gated as in Extended Data Fig. 9d; blue) isolated from spleens of B6.*Rag1*$^{-/-}$ mice 6-weeks post-naïve T cell congenic co-transfer. Background Rh123 efflux in CD45.1 B6 Teff cells treated with the MDR1 inhibitor, elacridar, is shown in gray. Representative of a total of 22 mice analyzed over two-independent T cell transfer experiments. *Right*, mean normalized Rh123 efflux (± SEM) in congenically-transferred CD45.1 wild type (B6; n = 7) or CD45.2 CAR-deficient (B6.*Nr1i3*$^{-/-}$; n = 8), PXR-deficient (B6.*Nr1i2*$^{-/-}$; n = 7) or CAR/PXR double-deficient (B6.*Nr1i3*$^{-/-}$*Nr1i2*$^{-/-}$; n = 7) spleen Teff cells, determined by flow cytometry as above. * P < .05, One-way ANOVA with Tukey's correction for multiple comparisons. **(b)** Mean relative *Abcb1a* expression (± SEM), determined by *ex vivo* qPCR, in CD45.1 wild type (B6; n = 9) or CD45.2 CAR-deficient (B6.*Nr1i3*$^{-/-}$; n = 9), PXR-deficient (B6.*Nr1i2*$^{-/-}$; n = 5) or CAR/PXR double-deficient (B6.*Nr1i3*$^{-/-}$*Nr1i2*$^{-/-}$; n = 7) spleen Teff cells (sorted as in Extended Data Fig. 9d) from spleens of congenically-transferred B6.*Rag1*$^{-/-}$ as in (a). * P < .05, One-way ANOVA with Tukey's correction for multiple comparisons.

Extended Data Figure 4. Blocking bile acid reabsorption attenuates weight loss induced by CAR-deficient T cells in *Rag*$^{-/-}$ mice. (a) Mean survival (*left*) or weight loss (*right*) (±SEM; n = 28) of co-housed B6.*Rag2*$^{-/-}$ mice transplanted with wild type (B6; blue; n = 15) or CAR-deficient (B6.*Nr1i3*$^{-/-}$; red; n = 13) naïve CD4^{+} T cells and treated with 2% (w:w) cholestyramine (CME) beginning at 3-weeks post-T cell transfer. **(b)** *Left*, H&E-stained sections of terminal ilea or colons from B6.*Rag2*$^{-/-}$ mice reconstituted with wild type or CAR-deficient T cells and treated +/- CME as in (a). Representative of 13 to 15 mice/group. *Right*, mean histology scores (± SEM; n = 13 to 15) for colons or terminal ilea as in (a). **(c)** Mean survival (*left*) or weight loss (*right*) (±SEM; n = 21/group) of co-housed B6.*Rag1*$^{-/-}$ mice lacking the ileal bile acid reuptake transporter, Asbt, after transplantation with wild type (B6; blue) or CAR-deficient (B6.*Nr1i3*$^{-/-}$; red) naïve CD4^{+} T cells. **(d)** *Left*, H&E-stained sections of terminal ilea or colons from Asbt-deficient B6.*Rag1*$^{-/-}$ mice reconstituted with wild type or CAR-deficient T cells as in (c). Representative of 21 mice/group. *Right*, mean histology scores (± SEM; n = 16) for colons or terminal ilea as above. NS, not significant, Two-way ANOVA.

Extended Data Figure 5. Commonalities between CAR-dependent gene expression in mucosal T cells and hepatocytes. (a) Venn diagrams showing overlap of differentially expressed genes between B6 wild type effector/memory (Teff) cells sorted from spleen, small intestine lamina propria (siLP) or colon lamina propria (cLP) of B6.*Rag1*$^{-/-}$ mice 3-weeks after naïve CD4^{+} T cell transfer (as in Fig. 2a). Genes increased or decreased in different comparisons are shown at *top* or *bottom*, respectively. **(b)** *Left*, volcano plots showing differentially expressed genes in primary mouse hepatocytes isolated from mice treated with or without either the selective

CAR agonist, TCPOBOP (TC), or the PXR agonist, PCN. Control mice received vehicle alone (corn oil (CO)). The number of genes increased (red) or decreased (blue) in the different comparisons are indicated. *Right*, venn diagrams showing overlap of genes significantly increased (*top*) or decreased (*bottom*) in hepatocytes from mice treated with TC or PCN. RNA-seq data in (b) were previously published (GSE104734)[18]; values reflect mean normalized expression, expressed as transcripts per million (TPM), from 3 mice per treatment condition. **(c)** Gene set enrichment analysis (GSEA) of genes selectively induced by TC treatment in mouse hepatocytes, defined as in (b), within genes differentially expressed between CAR-deficient (B6.*Nr1i3*$^{-/-}$) and wild type (B6) siLP Teff cells re-isolated from transferred B6.*Rag1*$^{-/-}$ mice 3-weeks after naïve CD4^{+} T cell transfer (as in Fig. 2a-c). Normalized enrichment score (NES) and associated *P* value are shown. **(d)** Volcano plot showing differential gene expression between CAR-deficient (B6.*Nr1i3*$^{-/-}$) and wild type (B6) siLP Teff cells re-isolated from transferred B6.*Rag1*$^{-/-}$ mice. Subsets of genes where CAR-occupancy is observed by ChIP-seq in hepatocytes from TC-treated mice (blue)[20]; where expression is selectively induced by TC, but not PCN, treatment in mouse hepatocytes (as in (b); purple); or both (red) are highlighted. Chi-square *P* values are shown. **(e)** CAR-occupancy, determined by ChIP-seq, at representative loci whose expression is regulated by CAR in both mucosal T cells and hepatocytes within mouse hepatocytes ectopically expressing epitope-tagged mouse (m) or human (h) CAR proteins and re-isolated from mice after treatment with the mCAR agonist, TCPOBOP (TC), or the hCAR agonist, CITCO. *P < 0.00001; statistically significant binding peaks were called in MACS using base settings.

Extended Data Figure 6. CAR promotes effector T cell persistence and IL-10 expression in the small intestine. **(a)** Equal numbers of CD45.1 wild type (B6; blue) and CD45.2 CAR-deficient (B6.*Nr1i3*$^{-/-}$; red) naïve CD4^{+} T cells were transferred together into B6.*Rag1*$^{-/-}$ mice. Resulting effector (Teff) cells were FACS-purified 2- 4- or 6-weeks later from spleen, mesenteric lymph node (MLN), small intestine lamina propria (siLP), or colon lamina propria (cLP) for *ex vivo* functional analyses via flow cytometry. Gating hierarchy is shown from a sample of MLN mononuclear cells at 2-weeks post-T cell transfer; representative of 5 mice. **(b)** Percentages of live CD44^{hi} wild type (B6; CD45.1^{+}) or CAR-deficient (B6.*Nr1i3*$^{-/-}$; CD45.1^{-}) effector/memory (Teff) cells (gated as in (a)) in tissues of congenically co-transferred B6.*Rag1*$^{-/-}$ mice over time (as in (a)), determined by flow cytometry. Numbers indicate percentages; representative of 5 mice per tissue and timepoint. **(c)** Mean $\log_2$ fold-change (F.C.) of CAR-deficient (B6.*Nr1i3*$^{-/-}$) *vs.* wild type (B6) Teff cell percentages ($\pm$ SEM; $n = 5$) in tissues of congenically co-transferred B6.*Rag1*$^{-/-}$ mice over time (as in (a-b)), determined by *ex vivo* flow cytometry. **(d)** Percentages (indicated by numbers) of wild type (B6, CD45.1^{+}; blue) and CAR-deficient (B6.*Nr1i3*$^{-/-}$, CD45.1^{-}; red) naïve (CD62L^{hi}) CD4^{+} T cells after sorting and mixing, and prior to *in vivo* transfer into *Rag1*$^{-/-}$ mice (input Tnaive); representative of 3 mixtures used for analyzing resulting Teff cells at 2- 4- or 6-weeks post-transfer. **(e)** Intracellular IL-10 and IFNγ expression, determined by flow cytometry after

ex vivo (PMA+Inonomycin) stimulation, in wild type (B6, blue; *left*) or CAR-deficient (B6.*Nr1i3*$^{-/-}$, red; *right*) non-Th17 Teff cells, from tissues of congenically co-transferred B6.*Rag1*$^{-/-}$ mice over time (as in (a)). Numbers indicate percentages; representative of 5 mice per tissue and time point. Mean percentages **(f)** or numbers **(g)** (± SEM; *n* = 5) of IL-10-expressing wild type (B6, *left*) or CAR-deficient (B6.*Nr1i3*$^{-/-}$, *right*) Teff cells, determined by *ex vivo* flow cytometry (as in (e)), from tissues of congenically co-transferred B6.*Rag1*$^{-/-}$ mice over time. MLN, mesenteric lymph nodes; siLP, small intestine lamina propria; cLP, colon lamina propria.

Extended Data Figure 7. Infiltration of total and Th17-lineage CD4$^+$ T cells into small intestine lamina propria in the presence and absence of CAR. (a) Percentages of CD3$^+$CD4$^+$ T cell infiltration into tissues of B6.*Rag1*$^{-/-}$ mice transplanted with 1:1 mixtures of wild type and CAR-deficient naïve CD4$^+$ T cells (as in Extended Data Fig. 6a) over time. Numbers indicate percentages; representative of 5 mice per tissue and time point. **(b)** Mean numbers of CD3$^+$CD4$^+$ T helper (T_H) cells (± SEM; *n* = 5) in tissues of transferred B6.*Rag1*$^{-/-}$ mice over time, determined by flow cytometry as in (a). **(c)** Mean relative *ex vivo* CAR (*Nr1i3*), MDR1 (*Abcb1a*), *Cyp2b10*, or *Il10* gene expression (± SEM; *n* = 3), determined by qPCR, in wild type (B6) CD4$^+$ effector/memory (Teff) cells (sorted as in Extended Data Fig. 9d) from spleens of transferred B6.*Rag1*$^{-/-}$ mice over time. **(d)** Expression of RORγt and IL-17A, determined by intracellular FACS analysis after *ex vivo* (PMA+ionomycin) stimulation, in wild type (B6) or CAR-deficient (B6.*Nr1i3*$^{-/-}$) CD4$^+$ effector/memory (Teff) cells isolated from tissues of congenically co-transferred B6.*Rag1*$^{-/-}$ mice at 2-weeks post-transfer. Numbers indicate percentages; representative of 5 mice per tissue and time point. **(e)** Mean percentages of (± SEM; *n* = 5) of wild type (B6; blue) or CAR-deficient (B6.*Nr1i3*$^{-/-}$; red) RORγt$^+$IL-17A$^-$ Teff cells, determined by intracellular flow cytometry (as in (d)). * $P < .05$, paired two-tailed student's *t* test. MLN, mesenteric lymph nodes; siLP, small intestine lamina propria; cLP, colon lamina propria.

Extended Data Figure 8. CAR is required for anti-CD3-induced IL-10 expression in effector and regulatory T cell subsets in the small intestine. (a) *Top row*, expression of Foxp3 and RORγt, determined by intracellular staining after *ex vivo* (PMA+ionomycin) stimulation, in CD4$^+$CD44^{hi} cells from spleen (*left*) or small intestine lamina propria (siLP, *right*) of wild type (B6, blue) or CAR-deficient (B6.*Nr1i3*$^{-/-}$, red) mice injected with or without isotype control (IgG) or anti-CD3 antibody. *Bottom 4 rows*, expression of IL-10 and IL-17A in wild type or CAR-deficient spleen or siLP T cell subsets from mice treated +/- isotype control (IgG) or anti-CD3 antibodies. Cells were gated and analyzed by flow cytometry as above. Numbers indicate percentages; representative of 3 mice per group and genotype analyzed over 2-independent experiments. **(b-c)** Mean percentages of IL-10-expressing T cell subsets (± SEM; *n* = 3), gated and analyzed by *ex vivo* flow cytometry as in (a), in spleen **(b)** or siLP **(c)** T_H cell subsets from wild type (B6, blue) or CAR-deficient

(B6.*Nr1i3*$^{-/-}$, red) mice injected with or without isotype control (IgG) or anti-CD3 antibody. * $P < .05$, paired two-tailed student's *t* test; some *P* values are listed directly.

Extended Data Figure 9. Effects of TCPOBOP-mediated CAR activation in CD4$^+$ T cells *in vitro* and *in vivo*. (a) Mean weight loss (± SEM; $n = 5$/group) of co-housed B6.*Rag2*$^{-/-}$ mice transplanted with CAR-deficient (B6.*Nr1i3*$^{-/-}$) CD4$^+$ naïve T cells and maintained on a CA-supplemented diet with or without TC treatment. Weights are shown relative to 3-weeks post-transfer when TC treatments were initiated. NS, not significant. **(b)** H&E-stained sections of terminal ilea or colons from B6.*Rag2*$^{-/-}$ mice reconstituted with CAR-deficient T cells and treated as above and as indicated. Representative of 5 mice/group. **(c)** Mean histology scores (± SEM) for colons or terminal ilea as in (b). NS, not significant. **(d)** 1:1 congenic mixtures of CD45.1 wild type (B6; blue) and CD45.2 CAR-deficient (B6.*Nr1i3*$^{-/-}$; red) naïve CD4$^+$ T cells were transferred into B6.*Rag1*$^{-/-}$ mice. Resulting effector (Teff) cells were FACS-purified 3-weeks later from spleen. Sequential gating strategy for re-isolating wild type and CD45.2 CAR-deficient spleen Teff cells is shown. *Bottom left,* mean relative *Abcb1a*, *Cyp2b10*, or *Il10* expression (± SEM; $n = 4$), determined by qPCR, in *ex vivo*-isolated wild type (B6) or CAR-deficient (B6.*Nr1i3*$^{-/-}$) spleen Teff cells. These cells were used for *ex vivo* cell culture experiments in the presence or absence of small molecule ligands ((e-g) below). * $P < .05$, ** $P < .01$, paired two-tailed student's *t* test. **(e)** Mean relative expression (± SEM) of *Abcb1a* ($n = 4$), *Cyp2b10* ($n = 4$), or *Il10* ($n = 3$), determined by qPCR, in wild type (B6) or CAR-deficient (B6.*Nr1i3*$^{-/-}$) Teff cells isolated from transferred *Rag1*$^{-/-}$ mice (as in (d)) and stimulated *ex vivo* with anti-CD3/anti-CD28 antibodies (for 24 hr) in the presence or absence of titrating concentrations of the CAR agonist, TC. ** $P < .01$, *** $P < .001$, **** $P < .0001$, two-way ANOVA. **(f)** Mean relative expression (± SEM) of *Abcb1a* ($n = 4$), *Cyp2b10* ($n = 4$), or *Il10* ($n = 3$), determined by qPCR, in wild type (B6) or CAR-deficient (B6.*Nr1i3*$^{-/-}$) Teff cells isolated and stimulated as in (e) in the presence or absence of TC (10 μM), the mCAR antagonist 5α-Androstan-3β-ol (And; 10 μM), or both. ** $P < .01$, *** $P < .001$, **** $P < .0001$, one-way ANOVA with Tukey's correction for multiple comparisons. **(g)** Mean relative *Abcb1a*, *Cyp2b10*, or *Il10* expression (± SEM; $n = 5$), determined by qPCR, in wild type (B6) or CAR-deficient (B6.*Nr1i3*$^{-/-}$) Teff cells isolated and stimulated as in (e-f) in the presence or absence of TC (10 μM) or the selective mouse PXR agonist, PCN (10 μM). Data are presented as fold-change in mRNA abundance relative to vehicle-treated cells (DMSO for TC; ethanol for PCN). **** $P < .0001$, one-way ANOVA with Tukey's correction for multiple comparisons. NS, not significant.

Extended Data Figure 10. Non-bile acid components in bile activate CAR and are influenced by mucosal inflammation. (a) Mean TR-FRET signals (± SEM; $n = 3$) from recombinant CAR:RXR heterodimers, prepared and analyzed as in Fig. 3a, in the presence of diluent alone (PBS), 1 μM TCPOBOP (TC), 1% small intestine lumen content (siLC), 1% bile (from gallbladder), or 1% colon lumen content (cLC)—all from wild

type (B6) mice—or in the presence of titrating concentrations of individual bile acids (BAs). The 4 bars for BAs are: (1) diluent (DMSO) alone; (2) 10 μM; (3) 100 μM; and (4) 1000 μM. Values reflect means of 3-independent experiments using extracts from different wild type mice or different fresh preparations of BA species; each concentration from each individual experiment was run in triplicate. **** $P < .0001$, NS, not significant, one-way ANOVA with Tukey's correction for multiple comparisons. **(b)** *Left*, mean TR-FRET signals (± SEM; $n = 3$) from recombinant CAR:RXR heterodimers, as above, in the presence of diluent alone (PBS), or 1% siLC or cLC from steady-state wild type (WT) or *Rag1*$^{-/-}$ B6 mice. *Right*, mean TR-FRET signals (± SEM; $n = 3$) from recombinant CAR:RXR heterodimers, as above, in the presence of 1% siLC (yellow) or cLC (brown) from B6.*Rag1*$^{-/-}$ mice transplanted with mixtures of CD45.1$^+$ wild type and CD45.2$^+$ CAR-deficient naïve CD4$^+$ T cells 2- 4- or 6-weeks after T cell transfer. Dashed gray line indicates basal TR-FRET signal in the presence of diluent (PBS) alone. **** $P < .0001$, NS, not significant, one-way ANOVA with Tukey's correction for multiple comparisons.

Extended Data Figure 11. Effector/memory lineages and small bowel-homing receptor expression exert independent influences MDR1 expression in human T cells. (a) FACS-based identification of *ex vivo* human CD4$^+$ naive (Tnaive; CD25$^-$CD45RO$^-$; grey) or effector/memory (Teff; CD25$^-$CD45RO$^+$; red) cells from healthy adult donor PBMC. For improved purity of Th1, Th2, Th17 and Th17.1 cells (see below), CCR10-expressing Th22 cells were excluded. Right panel shows CCR6 expression in Tnaive (grey) or non-Th22 Teff cells (red); these were gated as CCR6$^+$ or CCR6$^-$ to enrich for Th17 and non-Th17 Teff lineages, respectively. **(b)** Expression of CCR4 and CXCR3 in CCR6$^-$ (non-Th17; *left*) or CCR6$^+$ (Th17; *right*) Teff cells identifies enriched CCR6$^-$CCR4^{lo}CXCR3^{hi} (Th1; orange), CCR6$^-$CCR4^{hi}CXCR3^{lo} (Th2; blue), CCR6$^+$CCR4^{hi}CXCR3^{lo} (Th17; green), and CCR6$^+$CCR4^{lo}CXCR3^{hi} (Th17.1; red) subsets. **(c)** Expression of integrin α4 (α4 int.; *top*) in Th2, Th1, Th17 and Th17.1 human Teff cells gated as in (a-b). Expression of integrin β7 (β7 int.) and CCR9 within α4 int$^-$ (*middle*) or α4 int$^+$ (*bottom*) Th2, Th1, Th17 or Th17.1 cells gated as above. (a-c) Representative of 9 independent experiments using PBMC from different healthy adult donors. **(d)** Percentages ($n = 9$) of α4$^+$β7$^+$CCR9$^+$ cells within *ex vivo* Th1, Th2, Th17, or Th17.1 Teff cells gated as in (a-c). Data from independent donors are connected by red lines. **(e)** MDR1-dependent Rh123 efflux in the indicated Th1, Th2, Th17, or Th17.1 Teff subsets gated based on expression of α4 int., β7 int., and/or CCR9 in the presence (grey) or absence (red) of elacridar. Representative of 8 independent experiments using PBMC from different donors. **(f)** Mean percentages (± SEM; $n = 8$) of Rh123^{lo} (MDR1$^+$) cells within Th1, Th2, Th17, or Th17.1 Teff subsets gated based on expression of α4 int., β7 int., and/or CCR9 as in (e). * $P < .05$, ** $P < .01$, *** $P < .001$, One-way ANOVA with Tukey's correction for multiple comparisons. ND, not detectable; NS, not significant.

REFERENCES

1 Hofmann, A. F. & Hagey, L. R. Key discoveries in bile acid chemistry and biology and their clinical applications: history of the last eight decades. *Journal of lipid research* **55**, 1553-1595, doi:10.1194/jlr.R049437 (2014).

2 Poupon, R., Chazouilleres, O. & Poupon, R. E. Chronic cholestatic diseases. *J Hepatol* **32**, 129-140 (2000).

3 Arab, J. P., Karpen, S. J., Dawson, P. A., Arrese, M. & Trauner, M. Bile acids and nonalcoholic fatty liver disease: Molecular insights and therapeutic perspectives. *Hepatology* **65**, 350-362, doi:10.1002/hep.28709 (2017).

4 Cao, W. *et al.* The Xenobiotic Transporter Mdr1 Enforces T Cell Homeostasis in the Presence of Intestinal Bile Acids. *Immunity* **47**, 1182-1196 e1110, doi:10.1016/j.immuni.2017.11.012 (2017).

5 Qatanani, M. & Moore, D. D. CAR, the continuously advancing receptor, in drug metabolism and disease. *Curr Drug Metab* **6**, 329-339 (2005).

6 Lazar, M. A. Maturing of the nuclear receptor family. *J Clin Invest* **127**, 1123-1125, doi:10.1172/JCI92949 (2017).

7 Ludescher, C. *et al.* Detection of activity of P-glycoprotein in human tumour samples using rhodamine 123. *British journal of haematology* **82**, 161-168 (1992).

8 Ai, H. W., Hazelwood, K. L., Davidson, M. W. & Campbell, R. E. Fluorescent protein FRET pairs for ratiometric imaging of dual biosensors. *Nature methods* **5**, 401-403, doi:10.1038/nmeth.1207 (2008).

9 Pols, T. W., Noriega, L. G., Nomura, M., Auwerx, J. & Schoonjans, K. The bile acid membrane receptor TGR5 as an emerging target in metabolism and inflammation. *J Hepatol* **54**, 1263-1272, doi:10.1016/j.jhep.2010.12.004 (2011).

10 Zhang, J., Huang, W., Qatanani, M., Evans, R. M. & Moore, D. D. The constitutive androstane receptor and pregnane X receptor function coordinately to prevent bile acid-induced hepatotoxicity. *J Biol Chem* **279**, 49517-49522, doi:10.1074/jbc.M409041200 (2004).

11 Cerveny, L. *et al.* Valproic acid induces CYP3A4 and MDR1 gene expression by activation of constitutive androstane receptor and pregnane X receptor pathways. *Drug Metab Dispos* **35**, 1032-1041, doi:10.1124/dmd.106.014456 (2007).

12 Wei, P., Zhang, J., Egan-Hafley, M., Liang, S. & Moore, D. D. The nuclear receptor CAR mediates specific xenobiotic induction of drug metabolism. *Nature* **407**, 920-923, doi:10.1038/35038112 (2000).

13 Evans, R. M. & Mangelsdorf, D. J. Nuclear Receptors, RXR, and the Big Bang. *Cell* **157**, 255-266, doi:10.1016/j.cell.2014.03.012 (2014).

14 Urquhart, B. L., Tirona, R. G. & Kim, R. B. Nuclear receptors and the regulation of drug-metabolizing enzymes and drug transporters: implications for interindividual variability in response to drugs. *Journal of clinical pharmacology* **47**, 566-578, doi:10.1177/0091270007299930 (2007).

15 Staudinger, J. L. *et al.* The nuclear receptor PXR is a lithocholic acid sensor that protects against liver toxicity. *Proc Natl Acad Sci U S A* **98**, 3369-3374, doi:10.1073/pnas.051551698 (2001).

16 Powrie, F., Correa-Oliveira, R., Mauze, S. & Coffman, R. L. Regulatory interactions between CD45RBhigh and CD45RBlow CD4+ T cells are important for the balance between protective and pathogenic cell-mediated immunity. *J Exp Med* **179**, 589-600 (1994).

17 Arnold, M. A. *et al.* Colesevelam and Colestipol: Novel Medication Resins in the Gastrointestinal Tract. *The American journal of surgical pathology*, doi:10.1097/PAS.0000000000000260 (2014).

18 Cui, J. Y. & Klaassen, C. D. RNA-Seq reveals common and unique PXR- and CAR-target gene signatures in the mouse liver transcriptome. *Biochim Biophys Acta* **1859**, 1198-1217, doi:10.1016/j.bbagrm.2016.04.010 (2016).

19 Tzameli, I., Pissios, P., Schuetz, E. G. & Moore, D. D. The xenobiotic compound 1,4-bis[2-(3,5-dichloropyridyloxy)]benzene is an agonist ligand for the nuclear receptor CAR. *Mol Cell Biol* **20**, 2951-2958 (2000).

20 Niu, B. *et al.* In vivo genome-wide binding interactions of mouse and human constitutive androstane receptors reveal novel gene targets. *Nucleic Acids Res* **46**, 8385-8403, doi:10.1093/nar/gky692 (2018).

21 Karwacz, K. *et al.* Critical role of IRF1 and BATF in forming chromatin landscape during type 1 regulatory cell differentiation. *Nat Immunol* **18**, 412-421, doi:10.1038/ni.3683 (2017).
22 Asseman, C., Mauze, S., Leach, M. W., Coffman, R. L. & Powrie, F. An essential role for interleukin 10 in the function of regulatory T cells that inhibit intestinal inflammation. *J Exp Med* **190**, 995-1004, doi:10.1084/jem.190.7.995 (1999).
23 Shouval, D. S. *et al.* Interleukin 1beta Mediates Intestinal Inflammation in Mice and Patients With Interleukin 10 Receptor Deficiency. *Gastroenterology* **151**, 1100-1104, doi:10.1053/j.gastro.2016.08.055 (2016).
24 Durant, L. *et al.* Diverse targets of the transcription factor STAT3 contribute to T cell pathogenicity and homeostasis. *Immunity* **32**, 605-615, doi:10.1016/j.immuni.2010.05.003 (2010).
25 Sano, T. *et al.* An IL-23R/IL-22 Circuit Regulates Epithelial Serum Amyloid A to Promote Local Effector Th17 Responses. *Cell* **163**, 381-393, doi:10.1016/j.cell.2015.08.061 (2015).
26 Wan, Q. *et al.* Cytokine signals through PI-3 kinase pathway modulate Th17 cytokine production by CCR6+ human memory T cells. *J Exp Med* **208**, 1875-1887, doi:10.1084/jem.20102516 (2011).
27 Gagliani, N. *et al.* Coexpression of CD49b and LAG-3 identifies human and mouse T regulatory type 1 cells. *Nat Med* **19**, 739-746, doi:10.1038/nm.3179 (2013).
28 Pan, X., Kent, R., Won, K. J. & Jeong, H. Cholic Acid Feeding Leads to Increased CYP2D6 Expression in CYP2D6-Humanized Mice. *Drug Metab Dispos* **45**, 346-352, doi:10.1124/dmd.116.074013 (2017).
29 Kliewer, S. A. *et al.* An orphan nuclear receptor activated by pregnanes defines a novel steroid signaling pathway. *Cell* **92**, 73-82 (1998).
30 Timsit, Y. E. & Negishi, M. CAR and PXR: the xenobiotic-sensing receptors. *Steroids* **72**, 231-246, doi:10.1016/j.steroids.2006.12.006 (2007).
31 Vitek, L. Bile acid malabsorption in inflammatory bowel disease. *Inflamm Bowel Dis* **21**, 476-483, doi:10.1097/MIB.0000000000000193 (2015).
32 De Calisto, J. *et al.* T-cell homing to the gut mucosa: general concepts and methodological considerations. *Methods Mol Biol* **757**, 411-434, doi:10.1007/978-1-61779-166-6_24 (2012).
33 Acosta-Rodriguez, E. V. *et al.* Surface phenotype and antigenic specificity of human interleukin 17-producing T helper memory cells. *Nat Immunol* **8**, 639-646, doi:10.1038/ni1467 (2007).
34 Ramesh, R. *et al.* Pro-inflammatory human Th17 cells selectively express P-glycoprotein and are refractory to glucocorticoids. *J Exp Med* **211**, 89-104, doi:10.1084/jem.20130301 (2014).
35 Maglich, J. M. *et al.* Identification of a novel human constitutive androstane receptor (CAR) agonist and its use in the identification of CAR target genes. *J Biol Chem* **278**, 17277-17283, doi:10.1074/jbc.M300138200 (2003).
36 Albenberg, L. G., Lewis, J. D. & Wu, G. D. Food and the gut microbiota in inflammatory bowel diseases: a critical connection. *Curr Opin Gastroenterol* **28**, 314-320, doi:10.1097/MOG.0b013e328354586f (2012).
37 Campbell, C. *et al.* Bacterial metabolism of bile acids promotes generation of peripheral regulatory T cells. *Nature* **581**, 475-479, doi:10.1038/s41586-020-2193-0 (2020).
38 Chen, M. L., Takeda, K. & Sundrud, M. S. Emerging roles of bile acids in mucosal immunity and inflammation. *Mucosal Immunol*, doi:10.1038/s41385-019-0162-4 (2019).
39 Hang, S. *et al.* Bile acid metabolites control TH17 and Treg cell differentiation. *Nature* **576**, 143-148, doi:10.1038/s41586-019-1785-z (2019).
40 Song, X. *et al.* Microbial bile acid metabolites modulate gut RORgamma(+) regulatory T cell homeostasis. *Nature* **577**, 410-415, doi:10.1038/s41586-019-1865-0 (2020).
41 Knott, S. R. V. *et al.* A computational algorithm to predict shRNA potency. *Mol Cell* **56**, 796-807, doi:10.1016/j.molcel.2014.10.025 (2014).
42 Chen, R. *et al.* In Vivo RNA Interference Screens Identify Regulators of Antiviral CD4(+) and CD8(+) T Cell Differentiation. *Immunity* **41**, 325-338, doi:10.1016/j.immuni.2014.08.002 (2014).
43 Fellmann, C. *et al.* An optimized microRNA backbone for effective single-copy RNAi. *Cell reports* **5**, 1704-1713, doi:10.1016/j.celrep.2013.11.020 (2013).

44 Kosiewicz, M. M. *et al.* Th1-type responses mediate spontaneous ileitis in a novel murine model of Crohn's disease. *J Clin Invest* **107**, 695-702, doi:10.1172/JCI10956 (2001).

45 Langmead, B. & Salzberg, S. L. Fast gapped-read alignment with Bowtie 2. *Nature methods* **9**, 357-359, doi:10.1038/nmeth.1923 (2012).

46 Zhang, Y. *et al.* Model-based analysis of ChIP-Seq (MACS). *Genome Biol* **9**, R137, doi:10.1186/gb-2008-9-9-r137 (2008).

47 Robinson, J. T. *et al.* Integrative genomics viewer. *Nat Biotechnol* **29**, 24-26, doi:10.1038/nbt.1754 (2011).

48 Patro, R., Duggal, G., Love, M. I., Irizarry, R. A. & Kingsford, C. Salmon provides fast and bias-aware quantification of transcript expression. *Nature methods* **14**, 417-419, doi:10.1038/nmeth.4197 (2017).

49 Ritchie, M. E. *et al.* limma powers differential expression analyses for RNA-sequencing and microarray studies. *Nucleic Acids Res* **43**, e47, doi:10.1093/nar/gkv007 (2015).

50 Wei, G. *et al.* Global mapping of H3K4me3 and H3K27me3 reveals specificity and plasticity in lineage fate determination of differentiating CD4+ T cells. *Immunity* **30**, 155-167, doi:10.1016/j.immuni.2008.12.009 (2009).

51 Yusuf, I. *et al.* Germinal center T follicular helper cell IL-4 production is dependent on signaling lymphocytic activation molecule receptor (CD150). *Journal of immunology* **185**, 190-202, doi:10.4049/jimmunol.0903505 (2010).

52 Suino, K. *et al.* The nuclear xenobiotic receptor CAR: structural determinants of constitutive activation and heterodimerization. *Mol Cell* **16**, 893-905, doi:10.1016/j.molcel.2004.11.036 (2004).

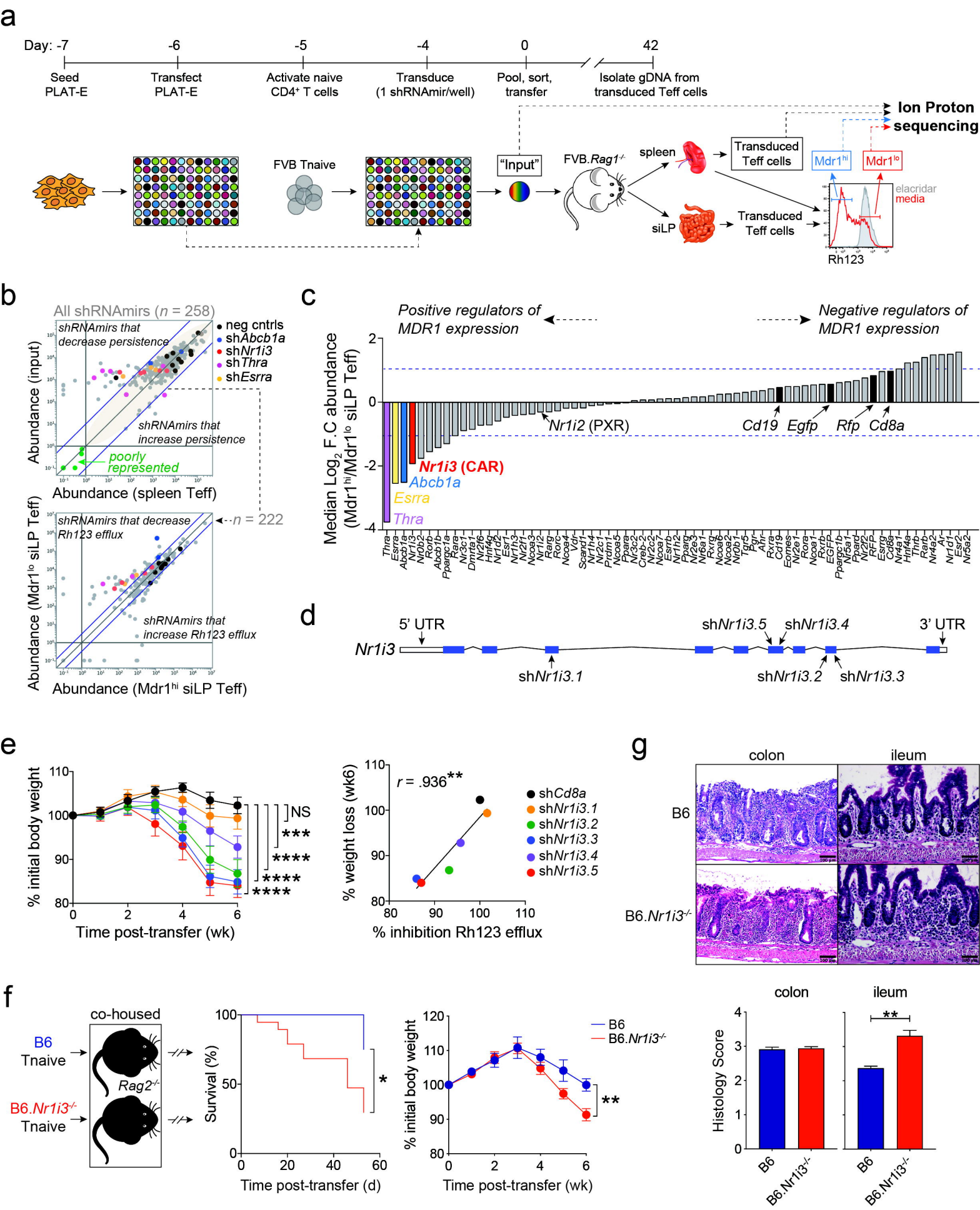
a
Day: -7
-6
-5
-4
0
42
Seed PLAT-E
Transfect PLAT-E
Activate naive CD4+ T cells
Transduce (1 shRNAmir/well)
Pool, sort, transfer
Isolate gDNA from transduced Teff cells
Ion Proton sequencing
FVB Tnaive
"Input"
FVB.Rag1-/-
spleen
siLP
Transduced Teff cells
Transduced Teff cells
Mdr1hi
Mdr1lo
elacridar
media
Rh123
b
All shRNAmirs (n = 258)
shRNAmirs that decrease persistence
shRNAmirs that increase persistence
poorly represented
neg cntrls
shAbcb1a
shNr1i3
shThra
shEsrra
Abundance (input)
Abundance (spleen Teff)
shRNAmirs that decrease Rh123 efflux
shRNAmirs that increase Rh123 efflux
n = 222
Abundance (Mdr1lo siLP Teff)
Abundance (Mdr1hi siLP Teff)
c
Positive regulators of MDR1 expression
Negative regulators of MDR1 expression
Median Log2 F.C abundance (Mdr1hi/Mdr1lo siLP Teff)
Nr1i2 (PXR)
Cd19
Egfp
Rfp
Cd8a
Nr1i3 (CAR)
Abcb1a
Esrra
Thra
d
5' UTR
3' UTR
Nr1i3
shNr1i3.1
shNr1i3.2
shNr1i3.3
shNr1i3.4
shNr1i3.5
e
% initial body weight
Time post-transfer (wk)
NS
***
****
****
****
% weight loss (wk6)
r = .936**
% inhibition Rh123 efflux
shCd8a
shNr1i3.1
shNr1i3.2
shNr1i3.3
shNr1i3.4
shNr1i3.5
g
colon
ileum
B6
B6.Nr1i3-/-
f
co-housed
B6 Tnaive
B6.Nr1i3-/- Tnaive
Rag2-/-
Survival (%)
Time post-transfer (d)
*
% initial body weight
Time post-transfer (wk)
B6
B6.Nr1i3-/-
**
colon
ileum
Histology Score
**
B6
B6.Nr1i3-/-
B6
B6.Nr1i3-/-

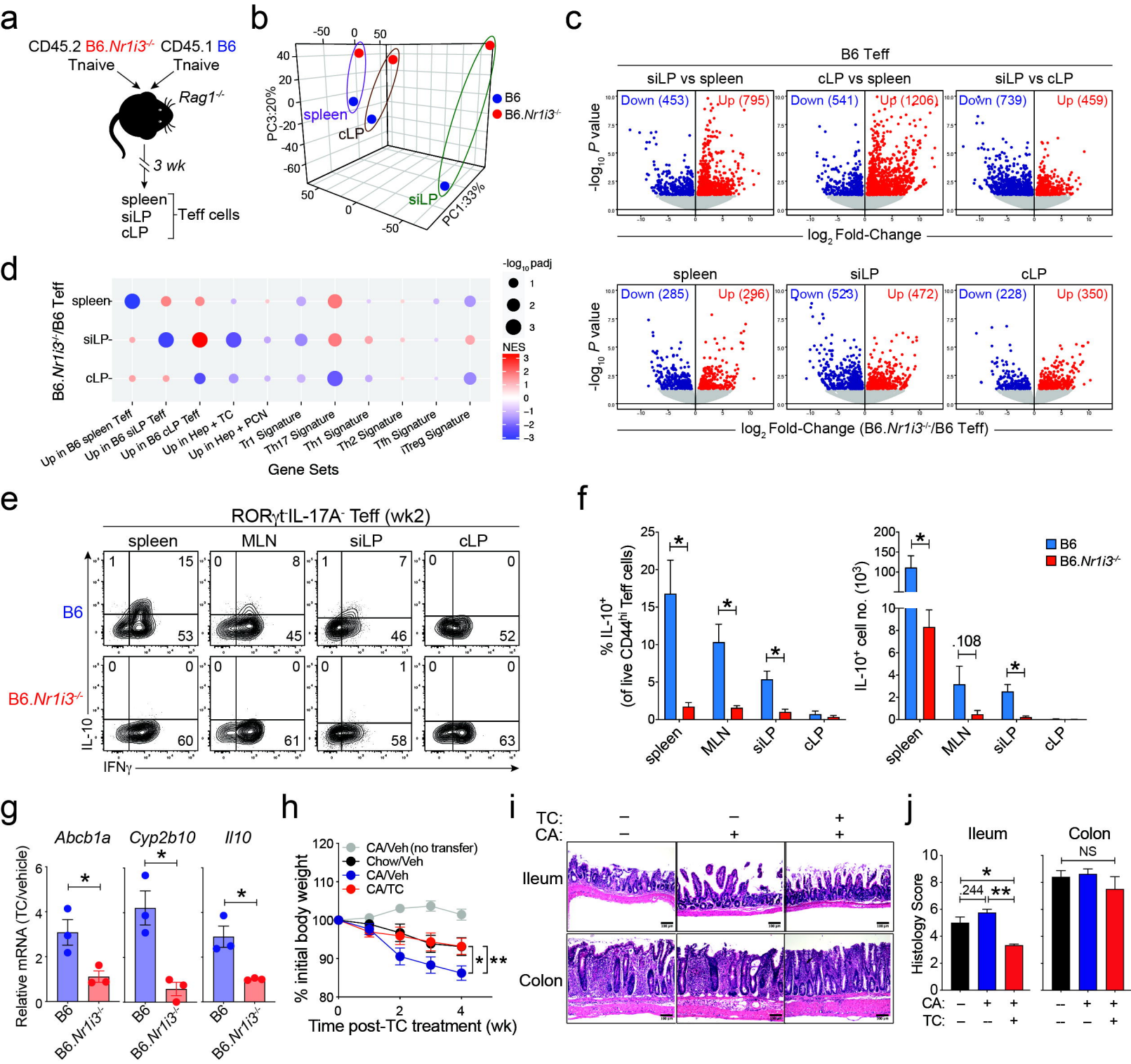
a
CD45.2 B6.Nr1i3-/- CD45.1 B6
Tnaive
Tnaive
Rag1-/-
3 wk
spleen
siLP
cLP
Teff cells
b
spleen
cLP
siLP
PC3:20%
PC1:33%
B6
B6.Nr1i3-/-
c
B6 Teff
siLP vs spleen
cLP vs spleen
siLP vs cLP
Down (453)
Up (795)
Down (541)
Up (1206)
Down (739)
Up (459)
-log10 P value
log2 Fold-Change
spleen
siLP
cLP
Down (285)
Up (296)
Down (523)
Up (472)
Down (228)
Up (350)
log2 Fold-Change (B6.Nr1i3-/-/B6 Teff)
d
B6.Nr1i3-/-/B6 Teff
spleen
siLP
cLP
-log10padj
NES
Up in B6 spleen Teff
Up in B6 siLP Teff
Up in B6 cLP Teff
Up in Hep + TC
Up in Hep + PCN
Tr1 Signature
Th17 Signature
Th1 Signature
Th2 Signature
Tfh Signature
iTreg Signature
Gene Sets
e
RORγt+IL-17A- Teff (wk2)
spleen
MLN
siLP
cLP
B6
B6.Nr1i3-/-
IL-10
IFNγ
f
% IL-10+ (of live CD44hi Teff cells)
IL-10+ cell no. (10^3)
B6
B6.Nr1i3-/-
.108
spleen
MLN
siLP
cLP
g
Abcb1a
Cyp2b10
Il10
Relative mRNA (TC/vehicle)
B6
B6.Nr1i3-/-
h
CA/Veh (no transfer)
Chow/Veh
CA/Veh
CA/TC
% initial body weight
Time post-TC treatment (wk)
i
TC:
CA:
Ileum
Colon
j
Ileum
Colon
Histology Score
.244
NS
CA:
TC:

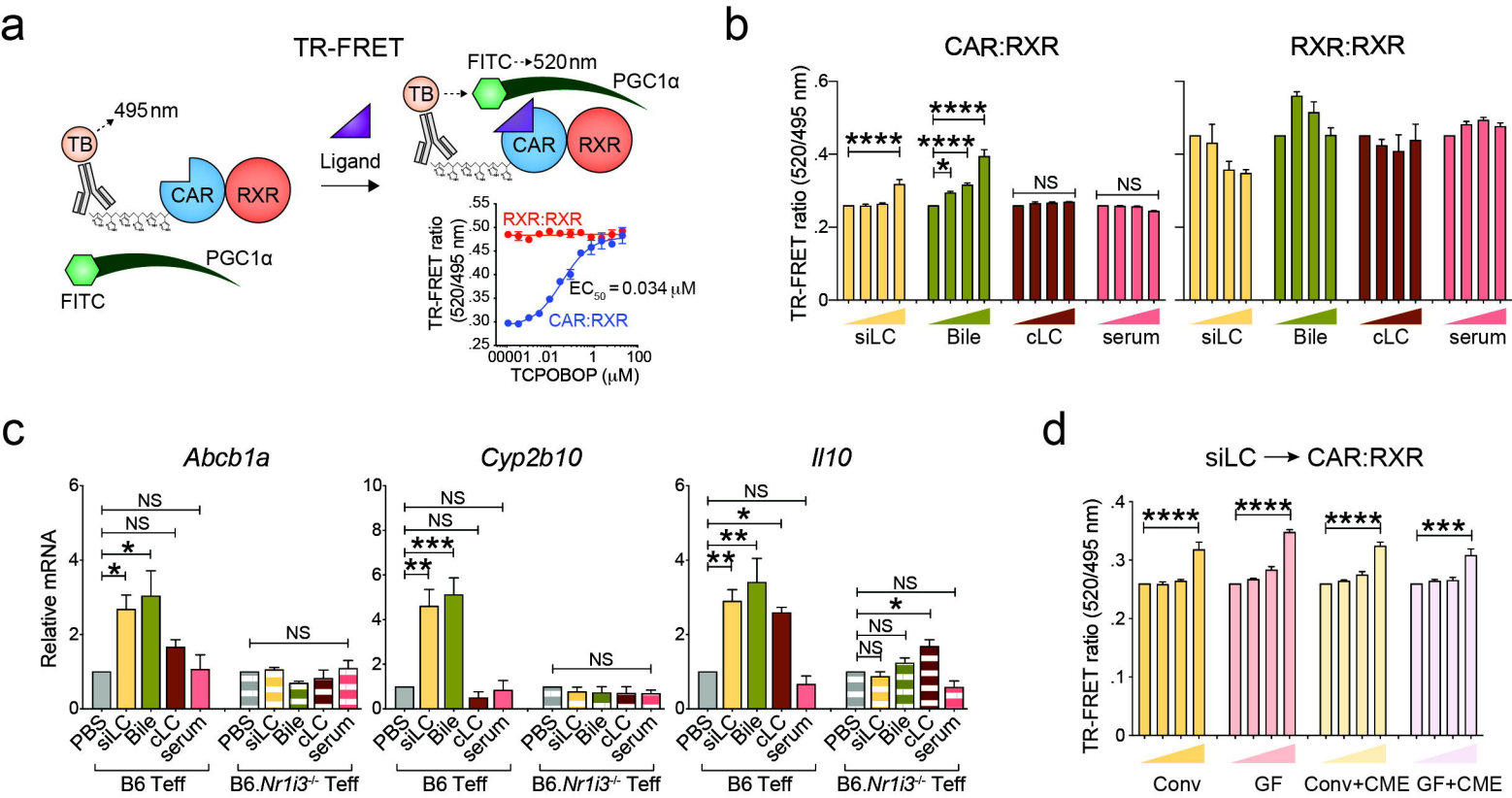
a
TR-FRET
495nm
TB
CAR
RXR
PGC1α
FITC
Ligand
FITC→520nm
TR-FRET ratio (520/495 nm)
RXR:RXR
CAR:RXR
EC50 = 0.034 μM
TCPOBOP (μM)
b
CAR:RXR
RXR:RXR
TR-FRET ratio (520/495 nm)
siLC
Bile
cLC
serum
NS
c
Abcb1a
Cyp2b10
Il10
Relative mRNA
PBS
B6 Teff
B6.Nr1i3-/- Teff
d
siLC → CAR:RXR
TR-FRET ratio (520/495 nm)
Conv
GF
Conv+CME
GF+CME

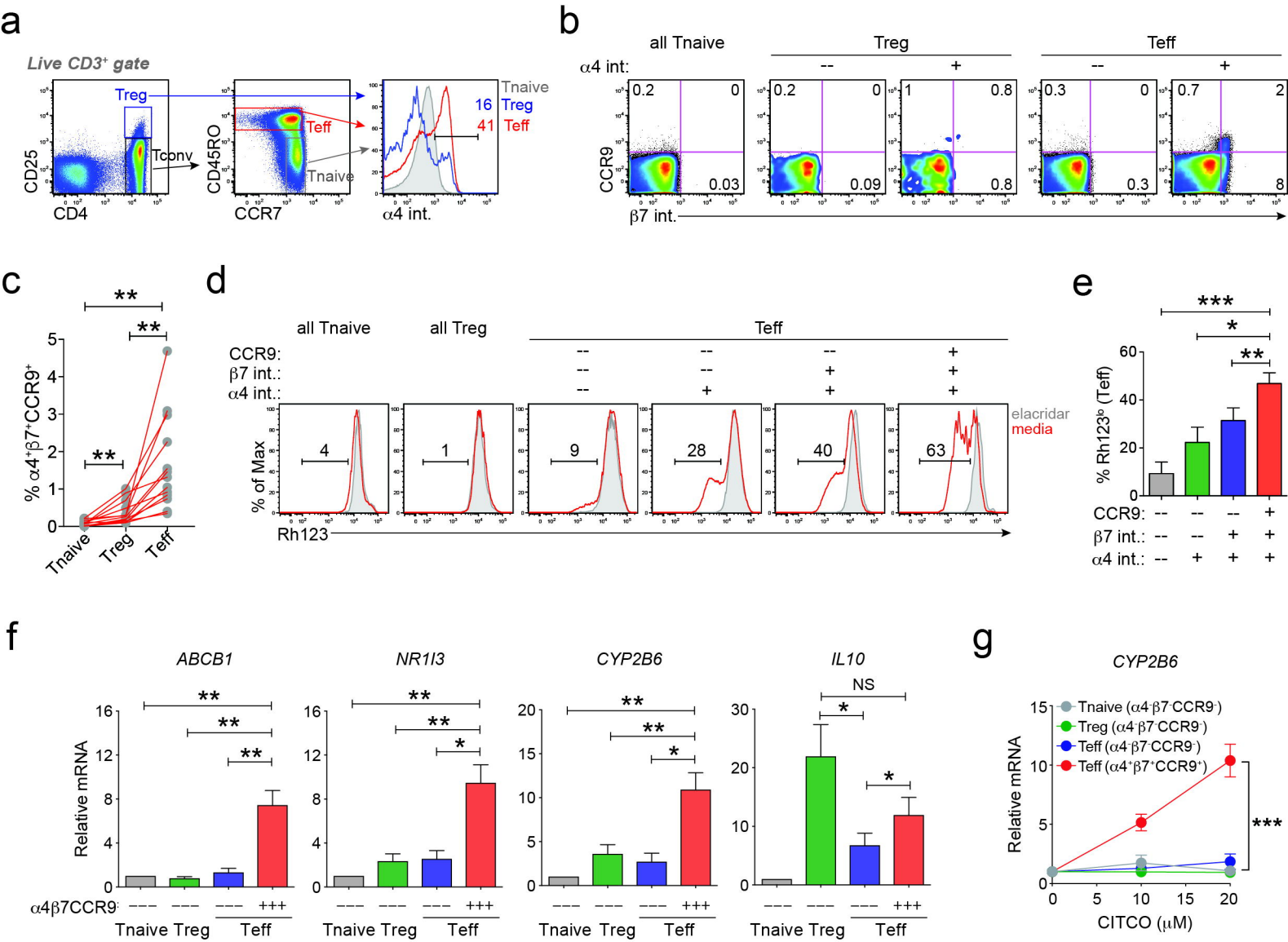
a
Live CD3+ gate
Treg
Tconv
CD25
CD4
Teff
Tnaive
CD45RO
CCR7
Tnaive
16
Treg
41
Teff
α4 int.
b
all Tnaive
Treg
Teff
α4 int:
--
+
CCR9
β7 int.
0.2
0
0.03
0.09
1
0.8
0.3
0.7
2
8
c
% α4+β7+CCR9+
Tnaive
Treg
Teff
d
all Tnaive
all Treg
Teff
CCR9:
β7 int.:
α4 int.:
% of Max
4
1
9
28
40
63
elacridar
media
Rh123
e
% Rh123lo (Teff)
CCR9:
β7 int.:
α4 int.:
f
ABCB1
NR1I3
CYP2B6
IL10
NS
Relative mRNA
α4β7CCR9:
Tnaive
Treg
Teff
g
CYP2B6
Tnaive (α4-β7-CCR9-)
Treg (α4-β7-CCR9-)
Teff (α4-β7-CCR9-)
Teff (α4+β7+CCR9+)
Relative mRNA
CITCO (μM)